HEALTH AND MEDICINE

Inhibition of fungal pathogenicity by targeting the H_2S-synthesizing enzyme cystathionine β-synthase

Wenqiang Chang[1]*, Ming Zhang[2], Xueyang Jin[1], Haijuan Zhang[3], Hongbo Zheng[1], Sha Zheng[1,4], Yanan Qiao[1], Haina Yu[1], Bin Sun[5], Xuben Hou[6], Hongxiang Lou[1]*

The global emergence of antifungal resistance threatens the limited arsenal of available treatments and emphasizes the urgent need for alternative antifungal agents. Targeting fungal pathogenic functions is an appealing alternative therapeutic strategy. Here, we show that cystathionine β-synthase (CBS), compared with cystathionine γ-lyase, is the major enzyme that synthesizes hydrogen sulfide in the pathogenic fungus *Candida albicans*. Deletion of CBS leads to deficiencies in resistance to oxidative stress, retarded cell growth, defective hyphal growth, and increased β-glucan exposure, which, together, reduce the pathogenicity of *C. albicans*. By high-throughput screening, we identified protolichesterinic acid, a natural molecule obtained from a lichen, as an inhibitor of CBS that neutralizes the virulence of *C. albicans* and exhibits therapeutic efficacy in a murine candidiasis model. These findings support the application of CBS as a potential therapeutic target to fight fungal infections.

INTRODUCTION

Fungal infections are a serious threat to human health and cause more than 1.6 million deaths annually (*1*). The rapid emergence of drug resistance poses a challenge for the management of fungal infections (*2*) and highlights the pressing need for alternative antifungal strategies. *Candida albicans*, a frequent human commensal fungal pathogen, can cause both mucosal and systemic candidiasis, the latter of which is potentially life-threatening. The pathogenic potential of *C. albicans* is determined by both the virulence factors and fitness attributes that allow it to infect a variety of host niches (*3*, *4*). Virulence factors include the morphological transition between the yeast and hyphal forms, phenotypic switching, adhesins, invasins, and secreted hydrolases, while fitness attributes include factors supporting cell growth, robust stress response systems, and cell wall remodeling capacities. Inhibition of either virulence factors or fitness attributes can reduce the pathogenicity of *C. albicans* (*3*, *4*).

Redox homeostasis is essential for host colonization by pathogens. To avoid oxidative killing by innate immune cells or environmental oxidants, *C. albicans* mounts oxidative stress responses (OSRs) by synthesizing small-molecule antioxidants and redox enzymes to promote its survival (*5*). Hydrogen sulfide (H_2S), an important endogenous molecule, has antioxidative properties and exerts a variety of biological actions, such as relaxing blood pressure in animals and protecting bacteria from antibiotics (*6*, *7*). H_2S-generating enzymes in mammals and in bacteria have been characterized, including cystathionine β-synthase (CBS), cystathionine γ-lyase (CSE), and 3-mercaptopyruvate sulfurtransferase (3MST) (*7*, *8*). CBS and CSE generate H_2S via the condensation of cysteine and homocysteine or α,β-elimination of cysteine, whereas 3MST reductively releases H_2S from 3-mercaptopyruvate (*7*, *8*). H_2S synthesized by CBS promotes the proliferation and migration of cancer cells and mediates ischemic stroke (*9*, *10*); thus, CBS inhibition has been considered as an option for treating cancer and stroke. In *C. albicans*, *CYS3* and *CYS4* are annotated in the *Candida* Genome Database as encoding CSE and CBS for synthesizing H_2S, respectively. However, their exact roles in synthesizing H_2S and physiological functions, particularly in fungal pathogenesis, remain elusive. To clarify the roles of these enzymes, we heterologously expressed Cys3 and Cys4 to determine their abilities to generate H_2S and constructed mutant strains to assess variations in fungal phenotype and pathogenicity.

In this study, we identified that Cys4 functions as a CBS and is the predominant H_2S-synthesizing enzyme in *C. albicans*. CBS determines fungal virulence by simultaneously participating in OSR, regulation of cell growth, hyphal elongation, and cell wall remodeling. Genetic disruption of *C. albicans* CBS results in low pathogenicity, suggesting that CBS is a promising antifungal target. We further obtained several CBS inhibitors by screening and elucidated the crystal structure of the catalytic core of *C. albicans* CBS (cCBS-cc). Protolichesterinic acid (PA), a lichen-derived small molecule as a CBS inhibitor, displayed therapeutic efficacy in a murine model of oropharyngeal candidiasis (OPC), supporting CBS as a potential therapeutic target for fighting fungal infections.

RESULTS

The CBS encoded by *CYS4* in *C. albicans* is a major source of H_2S generation

To characterize the roles of *C. albicans* Cys3 and Cys4 in generating H_2S, we heterologously expressed these proteins and performed in vitro enzyme assays. The results demonstrated that the ability of recombinant Cys4 to generate H_2S through two chemical reactions,

[1]Department of Natural Product Chemistry, Key Laboratory of Chemical Biology (Ministry of Education), School of Pharmaceutical Sciences, Cheeloo College of Medicine, Shandong University, Jinan, Shandong Province, China. [2]Institute of Medical Science, The Second Hospital, Cheeloo College of Medicine, Shandong University, Jinan, Shandong Province, China. [3]School of Pharmacy, Linyi University, Linyi, Shandong Province, China. [4]The Second Affiliated Hospital of Zhejiang Chinese Medical University, Hangzhou, Zhejiang Province, China. [5]National Glycoengineering Research Center, Shandong University, Jinan, Shandong Province, China. [6]Department of Medicinal Chemistry, Key Laboratory of Chemical Biology (Ministry of Education), School of Pharmaceutical Sciences, Cheeloo College of Medicine, Shandong University, Jinan, Shandong Province, China.
*Corresponding author. Email: changwenqiang@sdu.edu.cn (W.C.); louhongxiang@sdu.edu.cn (H.L.)

i.e., the reaction of L-cysteine with β-mercaptoethanol and the condensation of homocysteine with cysteine in the presence of the cofactor pyridoxal 5′-phosphate (PLP) (*11*), was over 500-fold higher than that of Cys3 (Fig. 1A). In addition, we found that these two enzymes catalyzed both types of reactions in the absence of exogenous PLP, although the activity was greatly reduced (fig. S1). These results suggest that CBS is the primary enzyme for H_2S biosynthesis in *C. albicans*.

To determine their functions at the cellular level, we constructed single-mutant and double-mutant strains of *cys3* and *cys4* using the Ura3-blaster method. These strains were named *cys3*Δ/Δ, *cys4*Δ/Δ, and *cys3*Δ/Δ *cys4*Δ/Δ. We generated the complemented strains *cys3*Δ/Δ + *CYS3* and *cys4*Δ/Δ + *CYS4* by inserting constructs of *CYS3* and *CYS4* under their native promoters in *cys3*Δ/Δ and *cys4*Δ/Δ, respectively. The wild-type strain CAF2-1 was used as a control strain. However, we failed to detect intracellular H_2S in situ because the H_2S content was below the detection limit when using both commercial and donated fluorescent H_2S-detecting probes (see Materials and Methods). Because of the short lifetime and low generation of H_2S in individual cells, we used a BiGGY (bismuth sulfite glucose glycine yeast) agar plate assay to measure the amounts of H_2S generated by the *C. albicans* cell population after a long period of growth. In BiGGY medium, bismuth ammonium citrate is reduced by H_2S donors, including NaHS and Na_2S, to produce a brown color but fails to react with glutathione, thiourea (Tu), and cysteine (fig. S2). Thus, this assay serves as a specific indicator of H_2S production. When grown in BiGGY medium, the brown color formed by the *cys4*Δ/Δ colonies was lighter than that of colonies of the wild-type strain or *cys4*Δ/Δ + *CYS4* (Fig. 1B), suggesting that the generation of H_2S is disrupted in *cys4*Δ/Δ. By contrast, disruption of *cys3* minimally affected H_2S generation (Fig. 1B). Because of the slow growth of *cys4*Δ/Δ on BiGGY agar plates (Fig. 1B), we increased the inoculum of *cys4*Δ/Δ to achieve a similar biomass to wild-type or *cys4*Δ/Δ + *CYS4* at the observation time point. The results showed that *cys4*Δ/Δ still generated less H_2S than the wild-type strain or *cys4*Δ/Δ + *CYS4* (Fig. 1B), further confirming that the CBS encoded by *CYS4* generates H_2S.

Both CBS and CSE participate in hydropersulfidation

CBS was recently reported to be involved in protein *S*-sulfhydration, a protective reaction that prevents the irreversible oxidation or electrophilic inactivation of thiol-containing proteins (*12*). Here, we found that recombinant Cys4 and Cys3 were both capable of transforming cystine to hydropersulfides in vitro (fig. S3A). We then used the fluorescent sulfane sulfur probe 4 (SSP4) to measure the intracellular levels of polysulfide in *cys3*Δ/Δ and *cys4*Δ/Δ. Microscopic inspection revealed that hydropersulfidation was not obviously affected in *cys3*Δ/Δ or *cys4*Δ/Δ but was severely disrupted in *cys3*Δ/Δ *cys4*Δ/Δ (fig. S3B).

CBS regulates the pathogenicity of *C. albicans*

Given its primary role in generating H_2S, we mainly focused on CBS in subsequent experiments. To confirm the antioxidative role of CBS, we first analyzed the intracellular reactive oxygen species (ROS) content in *cys4*Δ/Δ. As expected, *cys4*Δ/Δ exhibited increased intracellular ROS content, hypersusceptibility to H_2O_2 treatment and increased engulfment by macrophages (Fig. 1, C to E, and fig. S4). Consistent with the hydropersulfidation function of CSE in *C. albicans*, *cys3*Δ/Δ also displayed hypersusceptibility to H_2O_2 treatment and generated more ROS in response to H_2O_2 (Fig. S5). Reintegration of *CYS3* or *CYS4* under the control of its endogenous promoter partially restored the ability of *cys3*Δ/Δ or *cys4*Δ/Δ, respectively, to resist oxidative stress (Fig. 1E and fig. S5). Morphological tests revealed that *cys4*Δ/Δ was deficient in hyphal extension under multiple culture conditions and failed to form robust biofilms, whereas *cys3*Δ/Δ maintained the ability to form elongated hyphae (Fig. 1F and fig. S6).

Hyphal formation is an important virulence factor in *C. albicans* and is closely associated with its cell penetration ability and in vivo virulence. We therefore conducted a fungal invasion assay and an epithelial cell damage assay to determine the cell penetration ability of *cys4*Δ/Δ. The results showed that the ability of *cys4*Δ/Δ to invade and damage epithelial cells was compromised (fig. S7). Consistent with its reduced virulence in the in vitro test, *cys4*Δ/Δ was avirulent in a murine systemic infection model. Most of the *cys4*Δ/Δ-infected mice survived longer than 15 days even when infected at a dose four-fold greater than the commonly used inoculum. By contrast, mice infected with the wild-type strain at a dose equivalent to the commonly used inoculum (low) or four-fold greater (high) died within 5 days. Most of the mice infected with *cys4*Δ/Δ + *CYS4* also died within 8 days (Fig. 1G). Mice infected with a high dose of the wild-type strain did not survive more than 2 days, and therefore, mice infected with a low dose of the wild-type strain were used as the control in the fungal burden assay and histological examinations. At day 3 after infection, mice infected with *cys4*Δ/Δ had a notable lower fungal burden in the kidneys than mice infected with either wild-type strain or *cys4*Δ/Δ + *CYS4* (Fig. 1H). Moreover, compared with mice infected with the wild-type strain, *cys4*Δ/Δ-infected mice showed no visible filaments in the kidneys upon periodic acid–Schiff (PAS) staining and no obvious inflammatory influx upon hematoxylin and eosin (H&E) staining (Fig. 1I).

Deletion of CBS causes mitochondrial dysfunction in *C. albicans*

Given the antioxidant effect of H_2S, we speculated that intracellular H_2S functions as a reducing agent to mitigate oxidative stress during cell growth and, in particular, exposure to environmental stress. To test this hypothesis, we measured H_2S generation in *C. albicans* cells in response to oxidative stress using the BiGGY agar assay. As expected, oxidants such as H_2O_2 and menadione greatly reduced H_2S generation (Fig. 2A), suggesting that H_2S was consumed to neutralize oxidative stress. When sufficient antioxidants were supplied, intracellular H_2S was at least partially preserved (Fig. 2B). Mitochondria are the major site of ROS generation in cells, and ROS overproduction leads to mitochondrial dysfunction and intracellular redox imbalance. To determine whether the loss of H_2S generation and disrupted redox balance in *cys4*Δ/Δ affected mitochondrial respiration, we compared the growth curves of *cys4*Δ/Δ in yeast peptone dextrose (YPD) medium and in yeast peptone glycerol (YPG) medium. We found that *cys4*Δ/Δ exhibited slower growth when cultured with glycerol instead of dextrose as the carbon source in nutrient medium (Fig. 2C). This result suggested compromised mitochondrial respiration in *cys4*Δ/Δ, as the use of nonfermentable glycerol as the sole carbon source will enforce respiration to some extent. *cys4*Δ/Δ also showed increased mitochondrial membrane potential (mtΔΨ) (Fig. 2, D and E). The collapse of mtΔΨ using carbonyl cyanide *m*-chlorophenyl hydrazone (CCCP) enhanced ROS generation in *cys4*Δ/Δ (fig. S8). In addition, *cys4*Δ/Δ

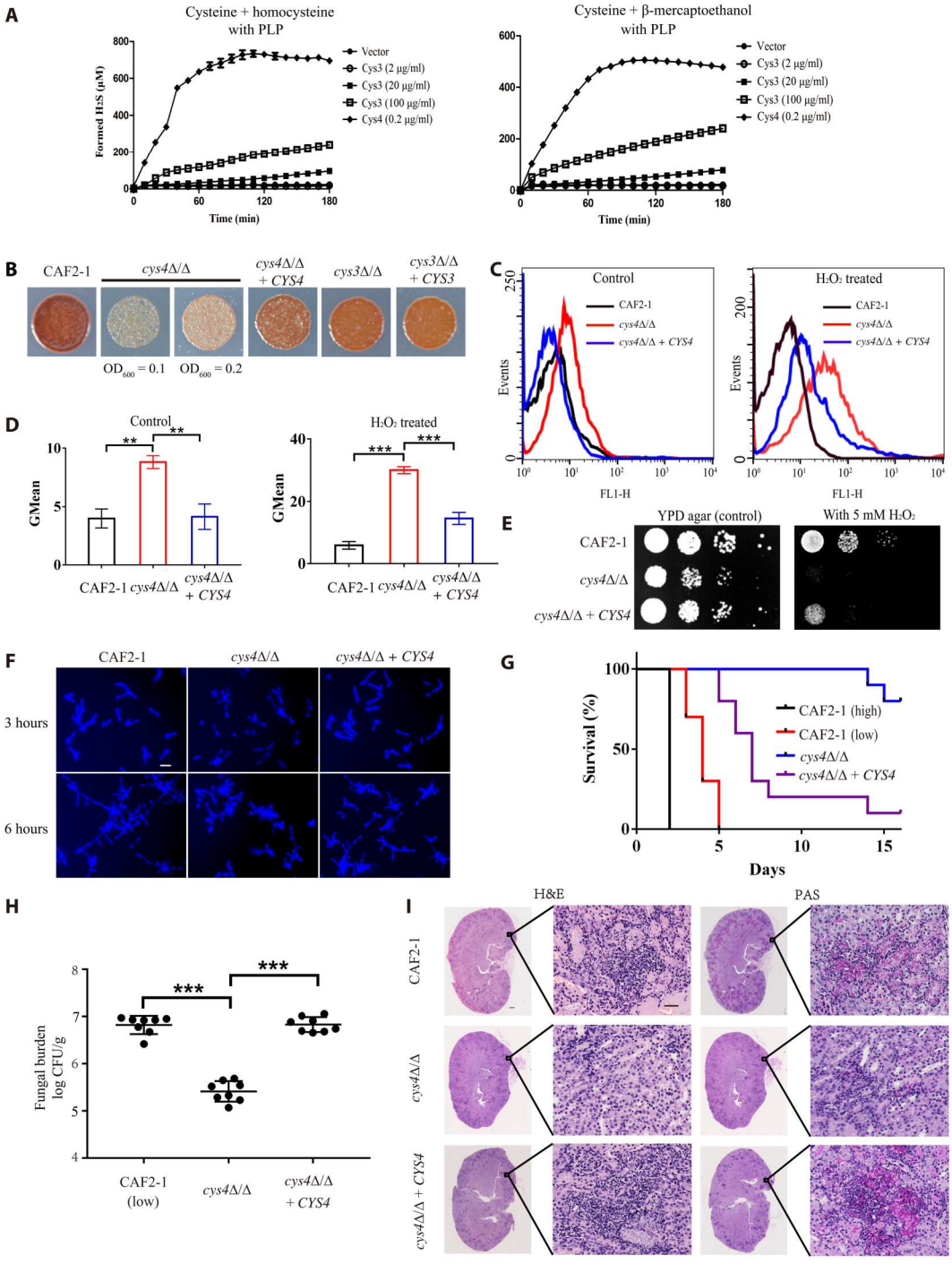

Fig. 1. The CBS encoded by *CYS4* regulates the virulence of *C. albicans*. (**A**) The ability of recombinant Cys4 or Cys3 to catalyze the generation of H_2S was assessed. (**B**) Measurement of H_2S generation by the indicated *C. albicans* strains. Strains were adjusted to a cell density of optical density at 600 nm (OD_{600}) = 0.1 and deposited on a BiGGY agar plate for 28 hours of growth. For *cys4*Δ/Δ, a cell density of OD_{600} = 0.2 was also used. (**C** and **D**) The indicated *C. albicans* strains were grown overnight and stained with the ROS probe 2',7'-dichlorodihydrofluorescein diacetate (DCFH-DA) to determine basal intracellular ROS levels in the absence of any stimulation or treated with 2 mM H_2O_2 for 6 hours. The fluorescence intensity was measured by flow cytometry (C), and geometric mean (GMean) values were calculated (D). (**E**) The susceptibility of *C. albicans* strains to H_2O_2 treatment was tested on yeast peptone dextrose (YPD) agar plates. (**F**) The hyphal elongation ability of *C. albicans* strains was visualized using CFW staining. Scale bar, 25 μm. (**G**) Survival of Balb/c mice infected with the indicated strains (n = 10 per group). Balb/c mice were infected with 5×10^5 colony-forming units (CFUs) (low) or 2×10^6 CFUs (high) of CAF2-1 or 2×10^6 CFUs of *cys4*Δ/Δ or *cys4*Δ/Δ + *CYS4* via the lateral tail vein. Mouse survival was monitored daily for 15 days. ***P < 0.001 for the *cys4*Δ/Δ-infected group versus CAF2-1 or the *cys4*Δ/Δ + *CYS4*-infected group. (**H**) Quantification of the fungal burden in kidney tissues of Balb/c mice at day 3 after infection with the indicated strain. (**I**) Staining of kidneys of Balb/c mice with H&E or PAS at day 3 after infection for microscopic observations. The log-rank test (G) and one-way analysis of variance (ANOVA) with Tukey's test (D and H) were used to determine statistical significance. **P < 0.01 and ***P < 0.001.

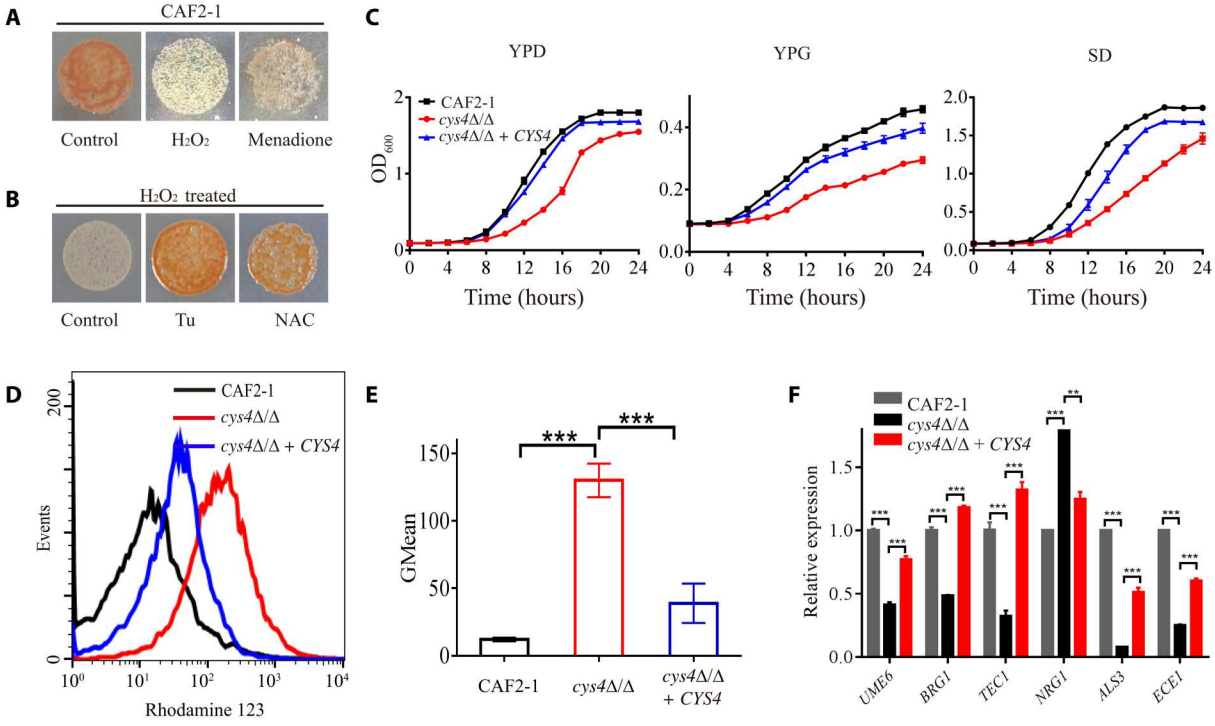

Fig. 2. CBS regulates OSR, mitochondrial function, cell growth, and hyphal extension of *C. albicans*. (**A**) The consumption of H_2S by *C. albicans* CAF2-1 in response to oxidative stress was detected using a BiGGY agar plate assay. *C. albicans* CAF2-1 was adjusted to a cell density of OD_{600} = 0.1 and deposited on a BiGGY agar plate containing H_2O_2 (5 mM) or menadione (2 mM) for 24 hours of growth. (**B**) Intracellular H_2S in *C. albicans* CAF2-1 was partially preserved in the presence of H_2O_2 (5 mM) when the antioxidant Tu (5 mM) or *N*-acetylcysteine (NAC) (5 mM) was provided. (**C**) Graphical representation of the growth of *C. albicans* cultured in YPD, YPG, or SD medium with an initial inoculated cell density of 10^5 cells/ml. (**D** and **E**) Quantification of the mtΔΨ of *C. albicans* strains. The fluorescence intensity of stained cells was measured by flow cytometry (D), and the GMean values of fluorescence intensity were calculated (E). (**F**) Transcription levels of hyphal transcriptional factors and adhesins in the indicated *C. albicans* strains cultured in RPMI 1640 medium for 5 hours at 37°C. 18*S rRNA* was used for data normalization. One-way ANOVA with Tukey's test [for (E) and (F)] was used to determine statistical significance. ***P* < 0.01, and ****P* < 0.001.

exhibited hypersusceptibility to respiratory inhibitors (fig. S9). Moreover, this hypersusceptibility was more pronounced in the presence of the alternative oxidase pathway inhibitor salicylhydroxamic acid (SHAM) (fig. S9), suggesting impaired classical electron transport chain (ETC) respiration in *cys4*Δ/Δ. The alternative oxidase pathway is considered as a branched respiratory pathway that provides alternative resistance to oxidative stress (*13*–*15*). This behavior of *cys4*Δ/Δ also mimics some characteristics of ETC-related mutants (*16*).

Deletion of CBS hampers the cell growth and hyphal elongation of *C. albicans*

Redox homeostasis is closely related to *C. albicans* cell growth, and ETC-related mutants with disrupted redox homeostasis exhibit defects in cell growth (*16*). Growth curve analysis revealed that *cys4*Δ/Δ exhibited a prolonged lag phase of growth compared with the wild-type strain or *cys4*Δ/Δ + *CYS4* in either YPD medium or synthetic medium plus dextrose (SD medium) (Fig. 2C).

In addition to retarded cell growth, morphotypic inspection revealed a defect in hyphal growth in *cys4*Δ/Δ (Fig. 1F and fig. S6). To address the mechanism by which CBS regulates hyphal elongation, we performed RNA sequencing (RNA-seq) of *cys4*Δ/Δ and the wild-type strain. Transcriptional profiling analysis revealed that filament- or biofilm-specific regulators, such as *UME6*, *TEC1*, and *BRG1*, and adhesins, such as the hypha-specific genes *ALS3* and *ECE1*, were down-regulated in *cys4*Δ/Δ compared with wild type, whereas the negative hyphal regulator *NRG1* was up-regulated (Fig. 2F, fig. S10A, and table S1).

Deletion of CBS results in cell wall remodeling in *C. albicans*

Mitochondrial dysfunction is related to cell wall remodeling in *C. albicans* (*17*, *18*), implying an alteration of cell wall components in *cys4*Δ/Δ. We also observed changes in the transcript levels of some cell wall synthesis genes in *cys4*Δ/Δ (Fig. 3A and fig. S10B). This evidence, together with the increased susceptibility of *cys4*Δ/Δ to cell wall-perturbing agents (fig. S9), indicated that cell wall integrity was compromised. The process of cell wall biogenesis and remodeling is regulated by several complex signaling pathways, such as mitogen-activated protein kinase (MAPK) cascades. Among these MAPK pathways, the Mkc1 MAPK cascade, which consists of Bck1-Mkk2-Mkc1, is primarily involved in cell wall biogenesis and responses to external cell wall stress, oxidative stimuli, and antifungal drugs (*19*). Compared with wild type or *cys4*Δ/Δ + *CYS4*, phosphorylation of Mkc1 was increased in *cys4*Δ/Δ at three time points within the first 24 hours of growth (Fig. 3B), indicating that the Mkc1 MAPK cascade is activated by *cys4* disruption. This further confirmed the disruption of cell wall integrity in *cys4*Δ/Δ and this strain's hypersusceptibility to cell wall stressors.

The cell wall comprises an inner skeletal layer of chitin and β-glucans and an outer layer of highly glycosylated mannoproteins.

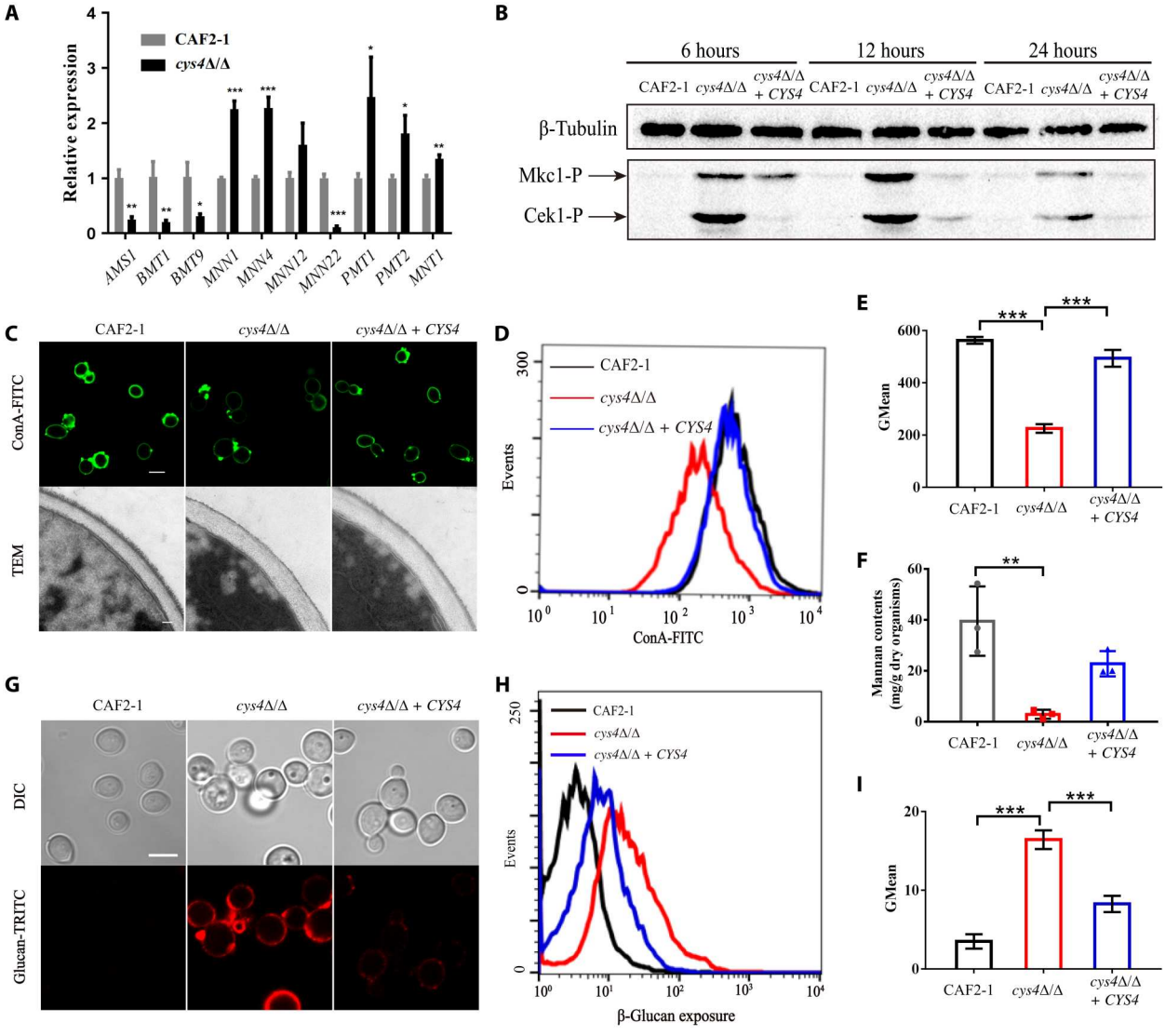

Fig. 3. CBS mediates the cell wall remodeling of *C. albicans*. (**A**) Transcriptional variations of several cell wall– and ER-related genes in *C. albicans* strains cultured in SD medium for 5 hours at 30°C. (**B**) Phosphorylated Mkc1 and Cek1 levels in the indicated *C. albicans* strains within 24 hours of growth in SD medium at 30°C. (**C** to **E**) The mannan content of the indicated strains was assessed using the concanavalin A–fluorescein isothiocyanate (ConA-FITC) staining method. Representative micrographs of ConA-FITC–stained samples are shown (C). Scale bar, 5 μm. Cell wall structures were also examined using transmission electron microscopy (TEM) (C). Scale bar, 100 nm (TEM). The fluorescence intensity of ConA-FITC was quantified by flow cytometry to determine the mannan content (D), and the GMean values of fluorescence intensity were calculated (E). (**F**) The mannan content in *C. albicans* was also measured using a chemical extraction method. (**G** to **I**) Surface β-glucan exposure in *C. albicans* strains. Cells of the indicated *C. albicans* strains were stained with an anti–β-1,3-glucan monoclonal antibody, followed by staining with a tetramethylrhodamine-5-(and-6)-isothiocyanate (TRITC)–labeled secondary antibody to visualize β-1,3-glucan by confocal microscopy. Representative micrographs of β-glucan exposure are shown (G). Scale bar, 5 μm. The fluorescence intensity was quantified by flow cytometry to indicate β-glucan exposure (H), and the GMean values were calculated (I). Student's *t* test (A) and one-way ANOVA followed by Tukey's test (E, F, and I) were used to determine statistical significance. **P* < 0.05, ***P* < 0.01, and ****P* < 0.001.

To uncover the influence of Cys4 on the fungal cell wall, we first evaluated cell wall composition. Genetic disruption of *cys4* reduced the yield of mannan, including phosphomannan but increased the proportion of chitin synthesis, probably to compensate for the decrease in mannan synthesis (Fig. 3, C to F, and fig. S11). These observations suggest that CBS is involved in regulating mannan synthesis. The compromised synthesis of mannan in the endoplasmic reticulum (ER) further increased the susceptibility of *cys4*Δ/Δ to the ER stressor dithiothreitol (DTT) (fig. S9).

Reduced mannan synthesis tends to increase β-glucan exposure, one of the most important pathogen-associated molecular patterns in *C. albicans*. β-Glucan is recognized by the myeloid-expressed Syk-coupled receptor Dectin 1 in innate immune cells (*20*). Increased β-glucan recognition can promote both phagocytosis and the production of proinflammatory cytokines, thereby effectively eradicating in vivo pathogens. Increased patchy binding of fluorescently labeled antibodies used to measure β-glucan around the cell periphery was observed in *cys4*Δ/Δ cells (Fig. 3G), indicating increased β-glucan exposure. However, the increase in β-glucan

exposure was greatly reversed in *cys4*Δ/Δ + *CYS4* (Fig. 3, G to I). Moreover, glucan exposure in *cys4*Δ/Δ was not affected by L-lactate (fig. S12), which promotes the masking of β-glucan (*21*), indicating that CBS is a valuable in vivo target for fungal recognition by immune cells. By contrast, increased glucan exposure was not detectable in *cys3*Δ/Δ (fig. S13). The Cek1 MAPK cascade has been suggested to control β(1,3)-glucan masking, and activation of this pathway increases β-glucan exposure in *C. albicans* (*22*). As expected, increased phosphorylation of Cek1 was observed in *cys4*Δ/Δ within 24 hours of growth compared with the wild-type strain or *cys4*Δ/Δ + *CYS4* (Fig. 3B), indicating that the disruption of *cys4* activates the Cek1 MAPK pathway.

CBS regulates the pathogenesis of *C. albicans* primarily by maintaining intracellular redox homeostasis

The *cys4*Δ/Δ strain exhibited impairments in resistance to oxidative stress, cell growth, and hyphal growth and increased β-glucan exposure. Because of the dominant role of CBS in H_2S generation and hydropersulfidation, we considered that these phenotypes of *cys4*Δ/Δ were likely attributable to loss of intracellular redox homeostasis. The transcriptional profiling and real-time quantitative polymerase chain reaction (qPCR) results indicated that a group of genes associated with redox homeostasis, including *CAT1* and *ERO1*, were differentially expressed when *cys4* was disrupted (Fig. 4A and fig. S10C). The catalase Cat1 and Cu/Zn superoxide dismutase Sod1 are two important enzymes in scavenging excess intracellular ROS. Ero1, an ER-resident flavoenzyme, mediates the formation of disulfide bonds for oxidative protein folding and plays an essential role in setting the redox potential in the ER. Given their critical roles in maintaining cellular redox homeostasis, we assessed the effects of ectopic overexpression of *CAT1*, *SOD1*, or *ERO1* in *cys4*Δ/Δ on susceptibility to H_2O_2. The compromised OSR in *cys4*Δ/Δ was at least partially rescued by ectopic overexpression of either antioxidant enzyme or the addition of the antioxidants Tu and *N*-acetylcysteine (NAC) (Fig. 4B and fig. S14). The generation of H_2S by these strains also greatly increased (Fig. 4C), probably because the increased antioxidant potential prevented the consumption of H_2S generated by other pathways.

To clarify whether the factors that mediate redox homeostasis are also involved in regulating cell growth, hyphal extension, and cell wall remodeling, we further evaluated the morphotypes of *cys4*Δ/Δ upon ectopic overexpression of *CAT1*, *SOD1*, or *ERO1*. Ectopic overexpression of either gene promoted cell growth and hyphal extension and greatly reversed the increase in β-glucan exposure in the *cys4* mutant (Fig. 4, D to I). In addition, we observed up-regulation of positive filament regulators, including both *TEC1* and *BRG1* in *cys4*Δ/Δ + *CAT1*, *cys4*Δ/Δ + *SOD1*, and *cys4*Δ/Δ + *ERO1* and *UME6* in *cys4*Δ/Δ + *ERO1* compared with the control strain *cys4*Δ/Δ + pBA1 (Fig. 4J). Accordingly, we observed that the in vivo pathogenesis of *cys4*Δ/Δ + *ERO1* and *cys4*Δ/Δ + *SOD1* was greatly increased compared with that of the *cys4* mutant (Fig. 4, K to M). These results suggest that the mediation of pathogenesis by Cys4 is dependent on intracellular redox homeostasis.

The metabolites generated by CBS are involved in regulating the virulence factor and fitness attributes of *C. albicans*

H_2S is an important metabolite generated by CBS. To characterize whether H_2S is the main factor regulating redox homeostasis to determine the phenotype of *cys4*Δ/Δ, we performed rescue experiments involving the exogenous addition of the H_2S donor NaHS or GYY4137. Exogenous addition of the H_2S donor partially rescued the defects of *cys4*Δ/Δ, including oxidative stress and hyphal growth, and reversed the increase in β-glucan exposure (fig. S15, A to G). Unexpectedly, addition of the H_2S donor had a minimal cell growth–promoting effect (fig. S15, H and I).

Another metabolite formed during the generation of H_2S is cystathionine, which is produced via the condensation of cysteine and homocysteine. CBS is also involved in the biosynthesis of cysteine via the transsulfuration pathway (*23*). To determine whether the loss of cystathionine and cysteine generation due to the absence of CBS activity is responsible for the phenotype of *cys4*Δ/Δ, we evaluated the effects of cystathionine and cysteine on *cys4*Δ/Δ. The addition of cystathionine or cysteine reduced the stimulation of mtΔΨ and ROS generation and promoted the hyphal growth (fig. S16, A to E). Exogenous cystathionine slightly promoted cell growth, whereas cysteine had a minimal effect on the growth of *cys4*Δ/Δ (fig. S16F). Both metabolites had minor effects on the β-glucan exposure of *cys4*Δ/Δ (fig. S16, G and H). Together, these results suggest that H_2S, cystathionine, and cysteine are important metabolites through which CBS regulates the pathogenicity of *C. albicans*.

The CBS inhibitor PA exhibits therapeutic efficacy in OPC

Aminooxyacetate (AOA) is a potent CBS inhibitor used in H_2S signaling studies and anticancer research. However, AOA is a nonspecific PLP-dependent enzyme inhibitor (*10*), and there is a need for potent and selective fungal CBS inhibitors. We therefore screened a chemical library comprising commercial synthetic compounds and natural small molecules to find fungal CBS inhibitors using AOA as a positive control. An enzyme assay using L-cysteine and L-homocysteine as substrates was adopted to monitor the inhibitory activities of the tested compounds. We obtained several hits that displayed much better activity than AOA, including PA isolated from an edible lichen, alternariol, and usnic acid (Fig. 5A and fig. S17). PA was the most potent *C. albicans* CBS inhibitor in terms of enzymatic activity, although its binding affinity for CBS was lower than that of AOA (Fig. 5, B and C). Because of the cellular impermeability of AOA, we synthesized a derivative, ethyl 2-(aminooxy)acetate (EAOA). The BiGGY agar assay revealed that both PA and EAOA reduced the H_2S generation of *C. albicans* at the cell population level, with stronger effects of PA than EAOA (Fig. 5D). Moreover, PA exhibited enzyme selectivity, as it inhibited CBS more potently than CSE (fig. S18) and fungal CBS more potently than human CBS (fig. S19). At the cellular level, only PA and EAOA resulted in *cys4*-deficient phenotypes in the wild-type strain in terms of hypersusceptibility to H_2O_2 treatment, retarded hyphal elongation and cell growth, and increased β-glucan exposure (Fig. 6, A to D, figs. S20 and S21, and table S2). However, glucan exposure did not increase further when the concentration of PA reached 64 μg/ml, probably because cell wall remodeling is an adaptation to stress in live cells, and the higher concentration of PA resulted in cell death. Consistent with this conclusion, cells

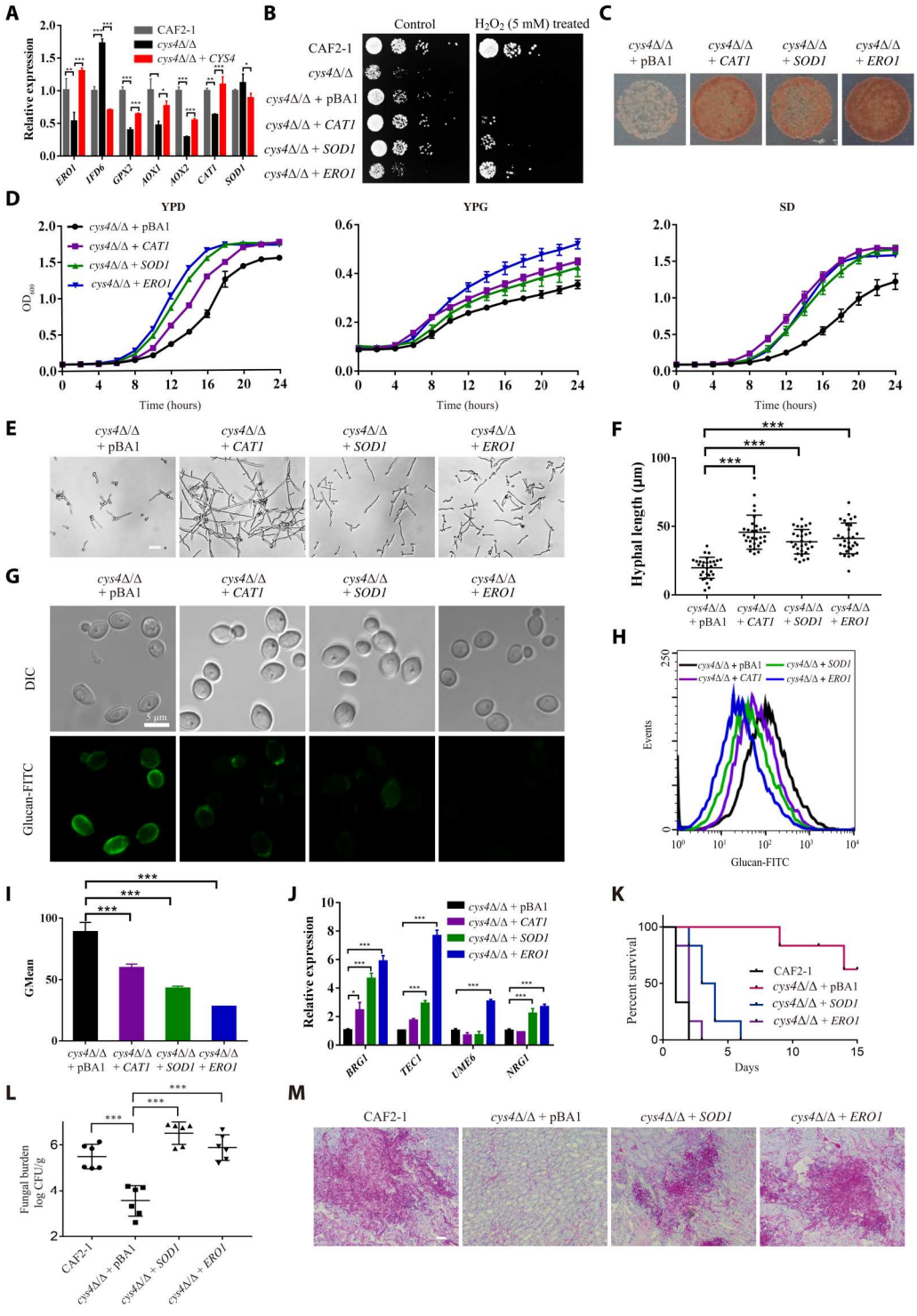

Fig. 4. CBS regulates the pathogenicity of *C. albicans* by maintaining intracellular redox homeostasis. (**A**) Transcription levels of several redox-related genes in the indicated *C. albicans* strains cultured in SD medium for 5 hours at 30°C. (**B**) The sensitivity of the indicated *C. albicans* strains grown on SD agar plates to H_2O_2 treatment. (**C**) Ectopic overexpression of *CAT1*, *SOD1*, or *ERO1* increased H_2S generation in *cys4* mutants. (**D**) Growth curves of indicated *C. albicans* strains cultured in YPD, YPG, or SD medium. (**E** and **F**) The hyphal elongation ability of *C. albicans* strains was visualized by a microscope after 6 hours of culture in RPMI 1640 medium (E). Scale bar, 20 μm. Filamentation was quantitatively assessed (F). (**G** to **I**) Ectopic overexpression of *CAT1*, *SOD1*, or *ERO1* reversed the increase in β-glucan exposure in the *cys4* mutant. Indicated *C. albicans* strains were stained with an anti–β-1,3-glucan monoclonal antibody, followed by staining with an FITC-labeled secondary antibody to visualize β-1,3-glucan by confocal microscopy (G). The fluorescence intensity was quantified by flow cytometry (H), and GMean values were calculated (I). (**J**) Transcriptional expression of hyphal regulators in *cys4*Δ/Δ + *CAT1*, *cys4*Δ/Δ + *SOD1*, and *cys4*Δ/Δ + *ERO1*. 18*S rRNA* was used for data normalization. (**K**) Survival of Balb/c mice infected with the indicated strains ($n = 8$ per group). Mice were infected with 2×10^6 CFUs of indicated strains for 15 days of observation. ***$P < 0.001$ for the *cys4*Δ/Δ + pBA1-infected group versus other groups. (**L**) Quantification of fungal burden in the kidney tissues of Balb/c mice infected with the indicated *C. albicans* strains at day 2 after infection. (**M**) The kidneys of infected mice were stained with PAS for microscopic observations. The log-rank test (K) and one-way ANOVA followed by Tukey's test (A, F, I, J, and L) were used to determine statistical significance. *$P < 0.05$, **$P < 0.01$, and ***$P < 0.001$.

exposed to PA (128 μg/ml) were killed and did not exhibit β-glucan exposure (Fig. 6B).

To evaluate the potential application of PA against other *Candida* species, we determined the minimum inhibitory concentration (MIC) of PA and the β-glucan exposure of *Candida* cells in the presence of PA. PA exhibited moderate inhibitory activity and elicited β-glucan exposure in *Candida glabrata*, *Candida parapsilosis*, and *Candida tropicalis* (table S2 and fig. S22), suggesting that inhibition of fungal CBS may be an alternative antifungal strategy for other *Candida* species as well. Furthermore, we observed that chemical conjugation of PA with the mitochondria-targeting moiety triphenylphosphonium cation (TPP^+) greatly improved its in vitro activity (fig. S23 and table S2), consistent with the primary location of CBS in mitochondria (*24*).

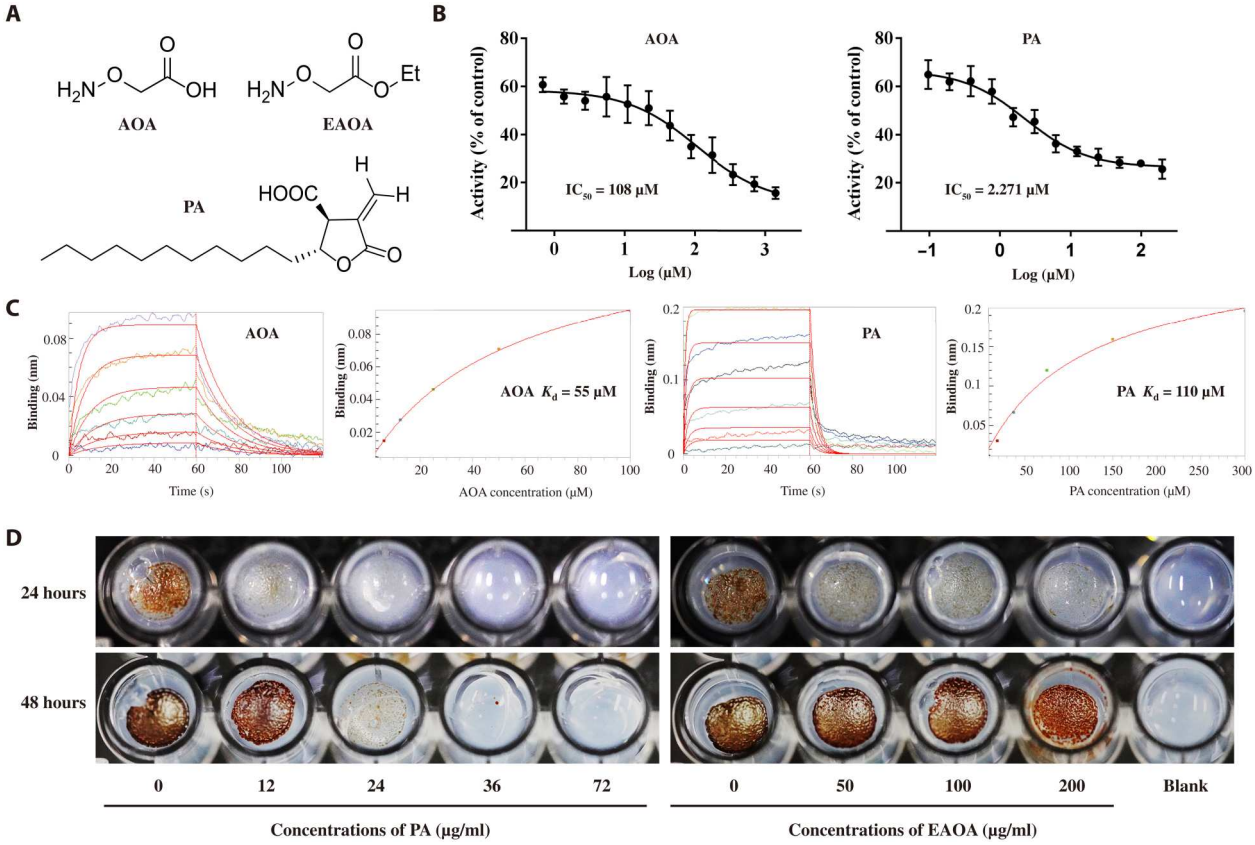

Fig. 5. Effects of fungal CBS inhibitors on enzyme activity. (**A**) Chemical structures of the CBS inhibitors AOA, EAOA, and PA. (**B**) Dose-dependent inhibition of *C. albicans* CBS activity by PA and AOA. (**C**) Kinetic binding sensorgrams of PA or AOA and steady-state fitting of the equilibrium responses versus compound concentrations based on a 1:1 binding model are shown. (**D**) The inhibition of H_2S generation by *C. albicans* by PA and EAOA as assessed by the BiGGY agar assay. *C. albicans* SC5314 cells were deposited on BiGGY agar containing different concentrations of PA or EAOA for 24 or 48 hours of growth and imaged by a camera.

To investigate the antifungal potential of PA in vivo, we evaluated PA in parallel with EAOA in a mouse model of azole-resistant OPC. PA or EAOA was added to the drinking water of the mice, and antifungal activity was assessed by measuring residual colony-forming units (CFUs) persisting on the tongue after 2 days of therapy. The average fungal burden decreased by more than 10-fold under PA or EAOA treatment (Fig. 6E). The decrease in fungal burden was confirmed by microscopic examination of PAS-stained tissue sections (Fig. 6F), which revealed that both PA and EAOA impaired the filamentation of *C. albicans*. The reduced fungal load and inhibition of hyphal formation in the infected tissue suggested therapeutic efficacy of PA in vivo.

The crystal structure of *C. albicans* CBS

To investigate the mode of interaction of PA with CBS, we prepared crystals of the cCBS-cc, which still maintains potent ability to generate H_2S and is inhibited by PA (fig. S24). We then elucidated the crystal structure of cCBS-cc (fig. S25 and table S3), which was used in homology modeling to obtain the intact structure of *C. albicans* CBS (available at https://doi.org/10.6084/m9.figshare.11919825). Further attempts to obtain the cocrystallized complex of cCBS-cc and PA were unsuccessful.

Complementation with a *CYS4* mutant fails to rescue most phenotypes of *cys4*Δ/Δ

Molecular docking of CBS and PA revealed that PA bound in the previously reported binding pocket for the cofactor PLP, which forms a Schiff base interaction with Lys^{53} (fig. S26, A and B) (*25*). Lys^{53} and Asn^{83} were identified as key amino acids that potentially influence the interaction between CBS and PA (fig. S26B). We hypothesized that these two residues also influence H_2S generation and other CBS functions. Therefore, we constructed two single mutants and a double mutant of CBS and performed enzyme assays. We found that the H_2S generation ability of Cys4 was greatly disrupted when Lys^{53} or Asn^{83} was individually mutated. The double mutant with K53A and N83A completely lost the ability to generate H_2S (fig. S26C). As expected, insertion of the mutant version of *CYS4* with double mutations into *cys4*Δ/Δ failed to reverse most of the phenotypes of *cys4*Δ/Δ, i.e., hypersensitivity to oxidative stress, retarded cell growth in YPD medium, defective hyphal growth, and increased β-glucan exposure (fig. S26, D to J). The exception was that *cys4*Δ/Δ complemented with the mutant version of *CYS4* exhibited slightly faster growth than *cys4*Δ/Δ in SD medium (fig. S26E).

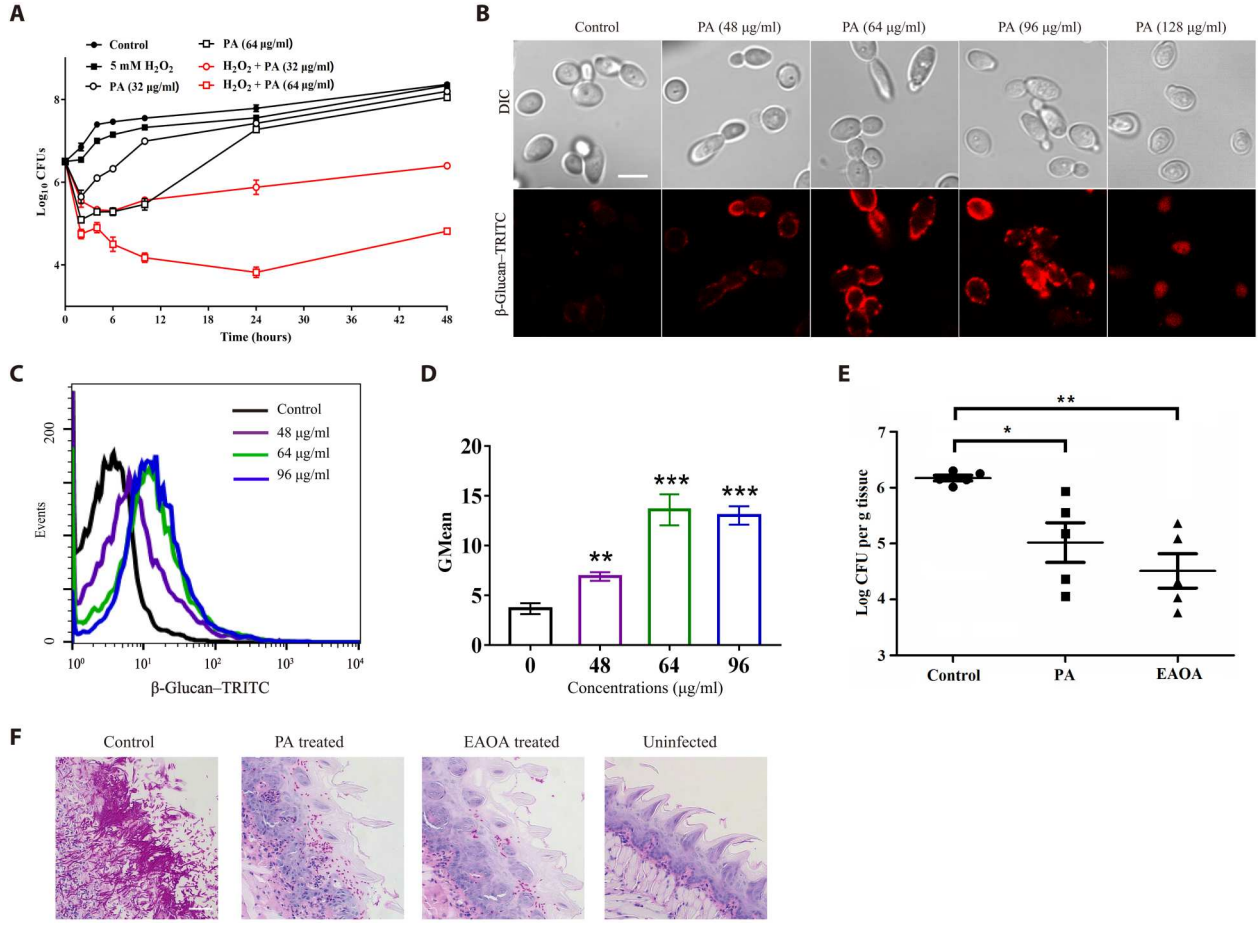

Fig. 6. Antifungal activities of CBS inhibitors in cells and animal models. (**A**) PA increased the fungicidal activity of H_2O_2 against *C. albicans*. (**B** to **D**) *C. albicans* CAF2-1 cells with an initial cell density of 10^7 cells/ml were treated with different concentrations of PA for 6 hours in SD medium. The β-glucan exposure of *C. albicans* was inspected by confocal microscopy (B). Scale bar, 5 μm. (C) The fluorescence intensity was quantified by flow cytometry to indicate β-glucan exposure. (D) The GMean values of fluorescence intensity were calculated. (**E** and **F**) PA and EAOA exhibited activity against azole-resistant *C. albicans* in a mouse model of OPC. The mice were infected sublingually with *C. albicans* 28A, an azole-resistant strain. PA (300 μg/ml) or EAOA (1 mg/ml) was added to drinking water after 1 day of infection (n = 5 per group). (E) Antifungal activity was assessed by measuring residual CFUs persisting on the tongue after 2 days of therapy. (F) Photomicrographs of PAS-stained tissue sections used to assess fungal morphology are presented. Scale bar, 50 μm. One-way ANOVA followed by Tukey's test was performed (D and E). *P < 0.05, **P < 0.01, and ***P < 0.001.

DISCUSSION

C. albicans has evolved multiple strategies to colonize diverse host niches, counteract host-imposed stresses, and avoid immune clearance. It can undergo the yeast-to-hyphae transition to invade epithelial cells and facilitate escape from immune cell attack (*26*). *C. albicans* can induce ROS-responsive transcription factors and stress-activated MAPK pathways to evade toxic ROS generated by the host immune system (*27*). In addition, it can rapidly adapt to environmental variation and modulate the cell wall architecture to avoid immune recognition by masking β-glucan (*21*, *26*). Yeast-to-hyphae switching is an important virulence factor that enables cell invasion, whereas factors enhancing OSR, supporting cell growth, and increasing glucan masking are fitness attributes that increase fungal adaptation in the host. Both virulence factors and fitness attributes are required for the pathogenicity of *C. albicans*, and inhibition of these factors can reduce its in vivo virulence. In this study, we identified that genetic or pharmaceutical inhibition of Cys4 function leads to defects in hyphal growth, deficiencies in resistance to oxidative stress, retarded cell growth, and increased β-glucan exposure, which, together, suppress the pathogenicity of *C. albicans*.

We first identified the CBS encoded by *CYS4* as a major H_2S-generating enzyme in *C. albicans*. The generation of H_2S by CBS is generally considered PLP dependent. However, we found that *C. albicans* CBS catalyzes two different reactions to generate H_2S without external addition of the cofactor PLP, most likely because the recombinant CBS has bound PLP during expression in the host *Escherichia coli*. This hypothesis is supported by the following lines of evidence. First, the purified Cys4 was yellow in color and exhibited an ultraviolet (UV)–visible absorption peak at 412 nm, which is characteristic of the protonated internal aldimine form of PLP (fig. S27). By contrast, the purified Cys4 with K53A and N83A mutations did not exhibit a yellow color because Lys^{53} forms the Schiff base interaction with PLP, and the absorption peak at 412 nm of this mutant was diminished compared with that of wild-type Cys4 (fig. S27). These features are also consistent with observations of

Mycobacterium tuberculosis CBS (*28*). In addition, a molecule of PO_4, which is part of PLP, was found in the active site of monomer A of our cCBS-cc structure after structural refinement. The ligand PO_4 occupied the same position in the cCBS-cc structure as the cofactor PLP in the structure of human CBS (fig. S25C), implying the presence of PLP in the cCBS-cc structure. The failure to observe intact PLP was likely due to the low quality of the electron density.

In addition to its role in producing H_2S, CBS drives protein *S*-sulfhydration, which is considered a protective mechanism for preventing the irreversible oxidation and inactivation of proteins (*12*, *29*). H_2S mediates protein *S*-sulfhydration via oxidized metal centers and oxygen under physiological conditions (*30*). These effects suggest that CBS regulates sulfhydration directly or indirectly through H_2S generation. The functional loss of CBS results in defects in both H_2S synthesis and sulfhydration to resist oxidative stress, suggesting a vital antioxidant role of CBS.

Growth defects are fitness deficits and are closely associated with fungal pathogenicity, as a slowly growing strain is more easily eliminated by the host's defenses. The growth phenotype of *cys4*Δ/Δ included a prolonged lag phase before the recovery of cell growth. Restoring intracellular redox homeostasis through ectopic overexpression of the antioxidant enzymes *CAT1*, *SOD1*, or *ERO1* shortened the lag phase and promoted cell growth of *cys4*Δ/Δ. This suggests that the growth regulation mediated by CBS is at least partially attributable to its antioxidant role.

C. albicans is able to grow in yeast, hyphal, and pseudo-hyphal forms. The hyphal form penetrates the epithelia and endothelia, causing tissue damage and allowing access to the bloodstream. Inhibiting hyphal formation reduces host colonization, increases immune elimination, and ultimately attenuates in vivo virulence (*26*). In this study, we found that CBS inhibition reduced hyphal extension and biofilm formation under multiple conditions. This regulatory mechanism was at least partially dependent on intracellular redox homeostasis and H_2S generation, as increasing H_2S generation via ectopic overexpression of *ERO1*, *SOD1*, or *CAT1* promoted the hyphal growth of *cys4* mutant by increasing the expression of hyphae-specific regulators, including *UME6*, *BRG1*, and *TEC1*.

The fungal cell wall comprises skeletal polysaccharides and numerous coated glycoproteins. The glycoproteins in *C. albicans* are highly glycosylated mannoproteins, and this glycosylation affects multiple aspects of fungal virulence, such as adhesion, morphogenesis, and immune recognition. Both protein folding and protein glycosylation participate in mannoprotein synthesis and mediate cell wall organization. Protein folding mediated by the oxidoreductin Ero1 is important for correct protein synthesis (*31*). In the *cys4*Δ/Δ strain, *ERO1* was down-regulated, which may cause unfolded or misfolded proteins to accumulate in the ER lumen and induce ER stress. This may explain the hypersusceptibility of *cys4*Δ/Δ to DTT, which is known to activate the unfolded protein response. The ER stress response stimulates the synthesis of H_2S, which, in turn, inactivates protein tyrosine phosphatase 1B through reversible sulfhydration to alleviate this stress (*32*). Therefore, the inhibition of H_2S synthesis in *cys4*Δ/Δ may accelerate the progression of ER stress and further affect correct protein synthesis.

Proper protein glycosylation is also important for protein folding, localization, and function (*33*). Members of the mannosyltransferase family participate in N-linked mannosylation, O-linked mannosylation, or phosphomannosylation of proteins in *C. albicans*, and these modifications play vital roles in fungal cell wall structure and cell surface recognition by the innate immune system (*34*). A variety of *C. albicans* mannosylation mutants are less pathogenic in vivo (*34*). In *cys4*Δ/Δ, compromise of *ERO1* and down-regulation of *AMS1*, *BMT1*, and *MNN22* were observed; these changes are associated with incorrect protein folding and reduced mannosylation. Deficient mannoprotein synthesis partially contributes to β-glucan exposure and increases Dectin-1–dependent immune recognition. In addition, *cys4*Δ/Δ exhibited abnormal respiration or mitochondrial dysfunction and increased β-glucan exposure, consistent with the downstream effects of inhibition of mitochondrial respiration reported in previous work (*18*). These observations suggest that blocking CBS is a potential strategy to combat *C. albicans* by abolishing mannoprotein synthesis and inducing cell wall remodeling.

In addition to its roles in generating H_2S and hydropersulfidation, CBS is involved in other processes of sulfur metabolism. It is difficult to holistically dissect the exact functions of CBS in governing the phenotype of *C. albicans*. H_2S, cysteine, and cystathionine are three important metabolites generated by CBS, and all contribute to the effects of CBS on the virulence factor and fitness attributes of *C. albicans*, although their phenotypic effects were less pronounced than expected. This is probably because it is difficult for exogenous supplementation to replace endogenously produced substances. In addition, there may be other unknown factors through which CBS regulates the pathogenicity of *C. albicans*.

The inhibition of CBS resulted in a disrupted intracellular redox state, growth defects, inhibited hyphal extension and biofilm formation, and increased β-glucan exposure, which together contributed to the low invasive ability of *C. albicans cys4*Δ/Δ and its elimination by immune cells. These results provide a valuable foundation for developing more potent fungal CBS inhibitors. Through high-throughput screening, we obtained a potent CBS inhibitor, PA, that inhibited CBS at the enzyme and cellular levels. Other inhibitors obtained by high-throughput screening were inferior to the positive control CBS inhibitor AOA or lost activity at the cellular level. Further evaluation using a murine OPC model supported the in vivo efficacy of PA as a CBS inhibitor, although neither PA nor EAOA showed obvious efficacy in the systemic candidiasis model, probably due to their potential in vivo toxicities via intraperitoneal injection. At a high dose of PA, a fungicidal effect was observed; this effect is largely unrelated to CBS inhibition because *cys4*Δ/Δ is viable. In addition, *cys4*Δ/Δ exhibited similar sensitivity to PA as the wild-type strain and *cys4*Δ/Δ + *CYS4* (table S2), implying the presence of other targets that are responsible for the growth inhibitory effect of PA. These results suggest that PA is not an ideal CBS inhibitor for drug development at present due to its off-target effects. However, the cellular phenotypes that mimicked those of the *cys4* mutant were caused by a low dose of PA. Moreover, PA showed a potent ability to inhibit fungal CBS, suggesting that PA still has potential as a lead compound for structural optimization to develop more specific and active fungal CBS inhibitors. To attempt to uncover the mode of interaction between PA and CBS, we further elucidated the crystal structure of cCBS-cc but unfortunately failed to obtain the cocrystallized complex of PA and cCBS-cc. Molecular docking indicated that PA binds in the previously reported binding pocket for the cofactor PLP. The mutation of key residues interacting with PA greatly disrupted the function of

CBS. These results provide a foundation for the future development of CBS inhibitors as antifungals.

In summary, we determined that fungal CBS affects multiple aspects of fungal pathogenicity: OSR, morphogenesis, cell wall remodeling, and cell growth. The simultaneous suppression of multiple pathogenicity factors through the genetic disruption of *cys4* or with small-molecule inhibitors is an attractive therapeutic strategy for combating fungal infections.

MATERIALS AND METHODS

Strains, growth conditions, and agents

C. albicans strains were propagated in YPD medium or supplemented with uridine (80 μg/ml) in an orbital shaker at 30°C. All *C. albicans* strains generated and used in this study are listed in table S4. SulfoBiotics SSP4 and the H_2S donor GYY4137 were purchased from Dojindo Company. The H_2S probe WSP5 was donated by M. Xian of Washington State University. (−)-Gallocatechin gallate was purchased from MedChemExpress. The fluorescent probes and antifungal drugs were purchased from Sigma-Aldrich. Other ordinary chemical reagents were purchased from Solarbio, Shanghai, China. Anti–phospho-p44/p42 MAPK (Thr^{202}/Tyr^{204}) antibody was purchased from Cell Signaling Technology (catalog no. 4370S). The antibody against β-tubulin was purchased from Abmart (Shanghai Co. Ltd., catalog no. M30109). The antibody against β-(1,3)-glucan was purchased from Biosupplies Inc. (Parkville, Australia, catalog no. 400-2). Fluoresceine isothiocyanate (FITC)–labeled goat anti-mouse antibodies were purchased from ZSBiO (Beijing, China, catalog no. ZF-0312) or from TransGen Biotech (Beijing, China, catalog no. HS211-01). Tetramethylrhodamine-5-(and-6)-isothiocyanate (TRITC)–labeled goat anti-mouse antibody was purchased from ZSBiO (Beijing, China, catalog no. ZF-0313).

Strain construction

*cys3*Δ/Δ, *cys4*Δ/Δ, and their double-mutant strains were generated in strain CAI4 using the Ura3-blaster approach. We generated reconstituted strains by inserting *CYS3* or *CYS4* constructs under their native promoters and named them *cys3*Δ/Δ + *CYS3* and *cys4*Δ/Δ + *CYS4*. Specifically, we cloned the up homologous sequences containing the open reading frame (orf) of *CYS3* or *CYS4* at Not I site and down homologous sequences at Apa I site in the plasmid pLNMCL (*35*) containing a *NAT1*-Clox cassette using an ExoCET DNA assembly method (*36*). The Not I–Apa I–excised fragments were used to transform *cys3*Δ/Δ or *cys4*Δ/Δ by electroporation to generate *cys3*Δ/Δ + *CYS3* and *cys4*Δ/Δ + *CYS4*, respectively. The *NAT1* of obtained positive colonies was excised through induction of Cre-mediated recombination. To insert the *CYS4* mutant with K53A and N83A into *cys4*Δ/Δ, the sequences containing the K53A and N83A mutations were first amplified from the *CYS4*-mutant plasmid constructed by GENEWIZ (Nanjing, China) and ligated with the fragments containing the remaining *CYS4* orf sequences and *NAT1*-Clox cassette from the *CYS4-NAT1*-Clox plasmid to form the *CYS4*-mutant-*NAT1*-Clox plasmid using a seamless cloning method based on the ClonExpress II One Step Cloning Kit (Vazyme Biotech, Nanjing, China, catalog no. C112-01). The constructed plasmid was confirmed by sequencing and excised by Not I–Apa I for transformation. To overexpress the catalase-encoding gene *CAT1*, the superoxide dismutase–encoding gene *SOD1*, and the ER-resident flavoenzyme–encoding gene *ERO1*, the orfs of these genes were amplified from the genome of CAF2-1 and cloned into pBA1 under the control of the constitutive *ADH1* promoter. The resulting plasmids and empty vector were used to transform *cys4*Δ/Δ. The *C. albicans cys4*Δ/Δ-*TDH3-RFP* strain was created by homologous recombination of red fluorescent protein (RFP) sequences into the 3′ end of the *TDH3*′ orf in *cys4*Δ/Δ. Correct chromosomal integration was verified by PCR diagnosis and/or DNA sequencing.

Cloning and functional characterization of Cys4 and Cys3

The full length of *CYS4* or *CYS3* gene was amplified from the genomic DNA of *C. albicans* SC5314 and cloned into the vector pET-32a(+) for expression as a fusion with an N-terminal Trx-S-His tag. After the sequence was confirmed, the vectors encoding *CYS4* or *CYS3* were used to transform *E. coli* BL21 (DE3). The cells harboring the plasmids were cultured to an optical density at 600 nm (OD_{600}) of 0.6 to 0.8 in LB broth medium containing ampicillin (100 μg/ml) at 37°C. Then, isopropyl β-D-1-thiogalactopyranoside was added to a final concentration of 0.1 mM to induce protein expression, and the cultures were incubated for an additional 16 to 20 hour at 16°C. All of the following processes were performed at 4°C. *E. coli* cells were collected and resuspended in 20 mM tris-HCl buffer (pH 8.0) containing 200 mM NaCl and 1 mM β-mercaptoethanol (buffer A). The cells were then homogenized by ultrasonication and centrifuged at 12,000 rpm for 50 min. The supernatant was passed through a Ni–nitrilotriacetic acid (NTA) column (GE Healthcare, USA) equilibrated with buffer A. Then, the resin was washed with buffer A containing 10 mM imidazole, and the recombinant protein was eluted with buffer A containing 250 mM imidazole. The protein concentration was calculated using Bradford reagent (Beyotime, Shanghai, China) with bovine serum albumin (BSA) as a standard. The purified protein was separated by SDS–polyacrylamide gel electrophoresis and visualized by Coomassie blue R250 staining.

H_2S-synthesizing enzyme activity assays were performed in 96-well plates as previously described (*11*). Briefly, the reaction mixture was incubated at 37°C and contained 200 mM Na/Bicine (pH 8.6), 50 μM PLP, BSA (0.25 mg/ml), 0.4 mM lead acetate, purified Cys3 or Cys4, and substrates: reaction 1 substrates (10 mM L-cysteine and 10 mM L-homocysteine) or reaction 2 substrates (10 mM L-cysteine and 10 mM β-mercaptoethanol). Purified pET-32a served as a negative control. In addition, similar reactions without PLP addition were performed. The reactions were continuously monitored by the increase in absorbance at 390 nm in a BioTek H1 plate reader. Quantitation of H_2S production was performed using a calibration curve obtained using NaHS under the same reaction conditions without substrates and purified enzyme.

Intracellular H_2S determination

Because the amount of H_2S generated by *C. albicans* was below the detection threshold using the lead acetate method, we used the H_2S-detecting fluorescent probe WSP5 (*37*) to measure H_2S. *C. albicans* cells were grown overnight in YPD medium, collected, washed with phosphate-buffered saline (PBS) three times, and diluted to 10^6 cells/ml. Hexadecyltrimethylammonium bromide (CTAB) at final concentrations ranging from 100 μM to 2 mM and WSP5 (200 μM) were added. A sample without WSP5 served as a negative control. The stained samples were analyzed by confocal microscopy

with excitation at 488 nm and emission in the range of 510 to 560 nm to detect the intracellular content of H_2S. We similarly used a commercial H_2S-detecting probe, AzMC, to detect intracellular H_2S in *C. albicans*. The stained samples were analyzed by confocal microscopy with excitation at 405 nm and emission in the range of 450 to 700 nm.

Detection of H_2S generation by *C. albicans* colonies

H_2S generation was detected using the BiGGY agar assay (Oxoid, England) (*38*). BiGGY is a medium containing bismuth ammonium citrate. H_2S reduces the bismuth ammonium citrate, resulting in a brown color. *C. albicans* strains were deposited on BiGGY agar plates. After the indicated incubation time at 30°C, the intensity of the brown color indicating H_2S generation was assessed.

Liquid chromatography–high-resolution mass spectrometry analysis of sulfidation products

The sulfidation reaction and persulfide detection were performed as previously described with slight modifications (*29*). Briefly, recombinant Cys3 (20 μg/ml) or Cys4 (20 μg/ml) was incubated with 4 mM L-cystine (CysSSCys) as the substrate in 100 mM Hepes buffer (pH 7.4) containing 50 μM PLP and 100 μM *S*-adenosyl methionine in a final volume of 1 ml. The reaction mixture was incubated at 37°C for 10, 20, 30, 60, 120, or 180 min. Control reactions lacking recombinant enzymes were run in parallel. The enzymatic reaction was terminated by adding a 5-volume excess of a methanol solution containing 5 mM Br-bimane. The mixtures were then incubated at 37°C for 20 min, followed by centrifugation (10,000*g* for 10 min) to collect the supernatants for liquid chromatography–high-resolution mass spectrometry (LC-HRMS) analysis. LC-HRMS detection was carried out on a Thermo Electron LTQ/Orbitrap XL hybrid mass spectrometer (Thermo Finnigan, Bremen, Germany) equipped with an electrospray ionization interface. Polysulfide derivatives were separated by reversed-phase high-performance LC (HPLC) on an Acclaim 120-C18 5-μm column (2.1 × 150 mm) with a linear 5 to 56% methanol gradient in 0.1% formic acid for 15 min at 25°C. A total flow rate of 0.2 ml/min and an injection volume of 10 μl were used. Ionization was achieved using electrospray in positive mode, and polysulfide derivatives were identified according to the multiple reaction monitoring parameters for bimane adducts as previously reported (*29*).

Polysulfide imaging

Cellular polysulfide imaging was performed using the commercial probe SSP4. Overnight-grown *C. albicans* cells were washed with PBS and then incubated with 50 μM SSP4 in PBS containing 1 mM CTAB at 37°C for 20 min. Cells that were not treated with SSP4 were used as negative controls. The cells were washed with PBS twice before fluorescence imaging at an excitation wavelength of 488 nm under a Zeiss LSM700 confocal laser microscope.

C. albicans phagocytic assay

The murine macrophage cell line RAW264.7 was cultured in Dulbecco's modified Eagle's medium supplemented with 2 mM glutamine, antibiotics [penicillin A (100 U/ml) and streptomycin (100 U/ml)], and 10% fetal bovine serum (FBS; HyClone, GA, USA) and maintained in a 37°C humidified incubator containing 5% CO_2 for 24 hours to form a monolayer of macrophages. Exponentially growing *C. albicans* cells were washed in PBS buffer and inactivated by UV light. A 100-μl volume containing 1×10^6 UV-inactivated cells was added to the macrophage monolayer. After 1.5 hours, the cells were washed twice and stained with Calcofluor White (CFW) for imaging using a confocal laser scanning microscope. The phagocytic index was assessed by counting the number of internalized yeast cells per at least 100 phagocytes.

Macrophage killing assay

RAW264.7 cells were cultured under the same conditions as described above for the phagocytic assay. A 100-μl volume containing 1×10^6 exponentially growing *C. albicans* cells was added to the macrophage monolayer. After incubation for 3 hours, excess unbound *C. albicans* cells were removed by rigorous washing with PBS. Macrophage killing was evaluated by trypan blue exclusion. Trypan blue (150 μl) and PBS (150 μl) were added to the cells, incubated for 2 min, and removed by gently washing twice with PBS; the cells were then fixed with 4% paraformaldehyde and counted under an inverted light microscope. Data were obtained in triplicate from at least three separate experiments by analyzing at least 100 macrophages per well.

C. albicans invasion assay

The human lung carcinoma epithelial cell line A549 was grown in RPMI 1640 medium supplemented with 10% FBS in a 37°C humidified incubator containing 5% CO_2 to form a confluent monolayer and then infected with *C. albicans* (1×10^5 yeast cells). After 2 hours of infection, the cell layers were washed with PBS three times. Samples were fixed in 2.5% (v/v) glutaraldehyde overnight at 4°C and postfixed in 1% (w/v) osmium tetroxide for 1 hour at room temperature. After fixing, the samples were dehydrated through a graded ethanol series before critical point drying (Polaron E3000, Quorum Technologies). The dried samples were mounted using carbon double-sided sticky discs on aluminum pins and gold-coated in an Emitech K550X sputter coater (Quorum Technologies). Images of the samples were recorded using a Quanta FEG-250 environmental scanning electron microscope (SEM) operating at 10 kV in high-vacuum mode.

Epithelial cell damage assay

A549 cells were used to assess cell injury caused by *C. albicans*. The release of lactate dehydrogenase (LDH) from epithelial cells into the surrounding medium was used as a measure of epithelial cell damage. A549 cells were cultured in RPMI 1640 medium supplemented with 10% FBS in a 37°C humidified incubator containing 5% CO_2. *C. albicans* cells (100 μl containing 1×10^5 cells) were applied to confluent monolayers of A549 cells in a 96-well plate, and the plate was incubated at 37°C and 5% CO_2 for 3 hours. Maximal LDH release was obtained by adding 15 μl of 0.9% Triton X-100 to the wells in the control set and vigorously disrupting the A549 cell layers with a pipette tip. Background LDH release was measured from nondisrupted A549 cell layers. Extracellular LDH activity was determined using an LDH cytotoxicity detection kit (Beyotime, China) according to the manufacturer's instructions. The percentage of cell lysis when challenged with *C. albicans* cells was calculated using the following formula: (experimental LDH release − background) / (mean maximal LDH release − background). All experiments were performed with four replicate wells of each treatment.

Murine model of disseminated candidiasis

BALB/c male mice (6 to 8 weeks old) were randomly assigned to test groups and infected with 5×10^5 or 2×10^6 CFUs of the indicated *C. albicans* strain in 200-μl saline suspensions via the lateral tail vein. Mouse survival was monitored daily. Three days after *C. albicans* infection, the mice were euthanized. Both kidneys were harvested; one kidney was processed for histopathological analysis, while the other was used for kidney fungal burden analysis. For histological analysis, the fixed kidney was embedded in paraffin, sectioned, and stained with PAS or H&E. The stained sections were examined microscopically for *C. albicans* morphology and infiltration.

C. albicans morphological examination

C. albicans cells were adjusted to 2×10^5 cells/ml in RPMI 1640 medium in 96-well flat-bottomed microtitration plates at 37°C without shaking. At the indicated time, the cells were photographed with an Olympus IX71 microscope. The length of individual filaments was measured using ImageJ software.

C. albicans biofilm formation evaluation

To assess the ability of *C. albicans* to form biofilms, overnight-grown *C. albicans* cells were inoculated in 96-well plates at an initial density of 1×10^6 cells/ml. After 24 hours of growth at 37°C, the nonadherent cells were aspirated, and the biofilms were washed with PBS twice. The biofilms were imaged by an Olympus IX71 microscope, and the viability of the biofilm cells was determined by Cell Counting Kit-8 (APExBIO, TX, USA) according to the manufacturer's protocol.

Analysis of biofilms by SEM

C. albicans cells were adjusted to 2×10^6 cells/ml in RPMI 1640 medium and grown on glass coverslips at 37°C for 24 hours. The supernatant was removed, and adherent cells were washed with PBS three times, fixed in 2.5% (v/v) glutaraldehyde overnight at 4°C, and postfixed in 1% (w/v) osmium tetroxide for 1 hour at room temperature. After fixing, the samples were dehydrated through a graded ethanol series before critical point drying (Polaron E3000, Quorum Technologies). The dried samples were mounted using carbon double-sided sticky discs on aluminum pins and gold-coated in an Emitech K550X sputter coater (Quorum Technologies). Images of the samples were recorded using a Quanta FEG-250 environmental SEM operating at 10 kV in high-vacuum mode.

RNA sample preparation and RNA-seq analysis

Overnight-grown *C. albicans* CAF2-1 and *cys4*Δ/Δ cells were diluted to 1×10^6 cells/ml in RPMI 1640 medium and cultured for 5 hours at 37°C. The cells were harvested by centrifugation and washed twice with PBS for RNA extraction. RNA was extracted using the RiboPure-Yeast Kit (Ambion) following the manufacturer's instructions. RNA purity was assessed using an Eppendorf BioSpectrometer. Each RNA sample had an A_{260}:A_{280} ratio between 1.8 and 2.0. RNA quality was analyzed in a 2100 Bioanalyzer system (Agilent Technologies) according to the manufacturer's instructions. RNA-seq was performed by Novogene (Beijing, China). Clustering of the index-coded samples was performed on the cBot Cluster Generation System using the TruSeq PE Cluster Kit v3-cBotHS (Illumina) according to the manufacturer's instructions. After cluster generation, the prepared libraries were sequenced on an Illumina HiSeq platform, and 150–base pair paired-end reads were generated. For data analysis, raw data (raw reads) in fastq format were first processed through in-house Perl scripts. Clean data or clean reads were obtained by removing reads containing adapters, reads containing poly-N, and low-quality reads from the raw data. Analysis of differential expression was performed using the DESeq R package (1.18.0). The *P* values were adjusted using the Benjamini and Hochberg method. Gene Ontology and Kyoto Encyclopedia of Genes and Genomes pathway analyses were implemented using the clusterProfiler R package. The RNA-seq data have been submitted to the Gene Expression Omnibus (GEO).

Validation of RNA-seq data

To validate the RNA-seq data, the expression levels of genes associated with filamentation (*NRG1*, *TEC1*, *UME6*, *BRG1*, *ECE1*, and *ALS3*) were determined by qPCR. One microgram of RNA used for RNA-seq was reverse-transcribed using ReverTraAce (Toyobo Co. Ltd., Osaka, Japan). Quantitative PCR was performed in an Eppendorf Mastercycler real-time PCR system using SYBR Green (Toyobo Co. Ltd.). The primers used in qPCR analysis are listed in table S5. The 18*S rRNA* gene was used for data normalization. The transcript levels of detected genes were calculated using the formula $2^{-\Delta\Delta CT}$.

The RNA-seq analysis revealed that the expression of genes associated with the OSR and cell wall synthesis was significantly altered. We then detected the expression levels of genes associated with the OSR (*ERO1*, *IFD6*, *GPX2*, *AOX2*, *AOX1*, *CAT1*, and *SOD1*) and mannan synthesis (*AMS1*, *BMT1*, *BMT9*, *MNN1*, *MNN4*, *MNN12*, *MNN22*, *PMT1*, *PMT2*, and *MNT1*) in *C. albicans* cells cultured in SD medium at 30°C for 5 hours. The actin gene (*ACT1*) was used for data normalization.

Antifungal susceptibility testing

The MIC_{80} values of the tested antifungal agents against *C. albicans* were determined by the broth microdilution procedure following CLSI M27-A3 guidelines (*39*).

Growth curves

Overnight grown *C. albicans* cells were used to inoculate into YPD, YPG, or SD medium with an initial cell density of 10^5 cells/ml. The cells were cultured at 30°C for 24 hours in a BioTek H1 plate reader, and the cell densities were determined by measuring the OD_{600} at 1-hour intervals.

Spot assays to test the susceptibility of *C. albicans* to cell stressors

Overnight-grown *C. albicans* cells were diluted to an OD_{600} of 0.1, and 3 μl of 1:10 serial dilutions was spotted onto YPD agar supplemented with cell wall–perturbing agents [caspofungin (0.2 μg/ml), CFW (50 μg/ml), Congo Red (50 μg/ml), and SDS (100 μg/ml)], osmotic stressors (1.5 M NaCl and 1 M sorbitol), respiratory inhibitors [rotenone (40 μM), an inhibitor of complex I; thenoyltrifluoroacetone (5 μM), an inhibitor of complex II; CCCP (20 μg/ml), an uncoupler of oxidative phosphorylation; NaN_3 (80 μg/ml), an adenosine 5′-triphosphate synthesis inhibitor; and SHAM (20 mM), an alternative oxidase (AOX) pathway inhibitor]; or DTT (20 mM; ER stressor) and incubated at 30°C. After 48 hours, the plates were photographed.

Measurement of ROS generation

ROS generation was quantified by 2′,7′-dichlorodihydrofluorescein diacetate (DCFH-DA). *C. albicans* cells were treated with or without H_2O_2 (2 mM) at 30°C for the indicated time. The cells were then stained with DCFH-DA (40 μg/ml) for 30 min in the dark and collected, and the fluorescence intensity was measured by flow cytometry. A total of 10,000 events were collected for data analysis without using specific gating strategies. The data were analyzed using FlowJo version 10 software.

Analysis of mtΔΨ

Rhodamine 123 (Rh123) was used to investigate the mtΔΨ of *C. albicans* in this study. *C. albicans* cells were stained with Rh123 (5 μg/ml) for 30 min in the dark and detected by flow cytometry. A total of 10,000 events were collected for data analysis without using specific gating strategies. The obtained data were analyzed using FlowJo version 10 software.

Alcian blue binding assay

Phosphomannan content was determined using an Alcian Blue affinity assay. Exponentially growing *C. albicans* cells (1.5×10^7) were washed with 0.02 M HCl and then incubated with Alcian blue (30 μg/ml) for 10 min at room temperature. The OD_{600} of the supernatant was measured, and the concentration of Alcian blue was determined by reference to a standard curve. The amounts of Alcian blue bound to *C. albicans* cells were calculated by subtracting the amounts of dye in the supernatant from the total used amounts.

Analysis of cell wall composition

C. albicans cells were grown in YPD medium at 30°C and broken with glass beads. The homogenate was centrifuged at 1000*g* for 10 min, and the pellet containing the cell debris and walls was washed with 1 M NaCl, resuspended in buffer [500 mM tris-HCl buffer (pH 7.5), 2% (w/v) SDS, 0.3 M β-mercaptoethanol, and 1 mM EDTA], boiled for 10 min, and freeze-dried. β-Glucan and mannan levels were hydrolyzed and quantified by measuring glucose and mannose, respectively. To quantify glucose and mannose, the cell walls were resuspended in 2 M trifluoroacetic acid, boiled for 3 hours, washed, and centrifuged at 21,500*g* for 10 min. The hydrolysates were analyzed by HPLC. For total protein determination, the cell walls were resuspended in 1 N NaOH, boiled for 30 min, neutralized with 1 N HCl, and assayed using the Bradford method.

Determination of chitin content in cell walls

C. albicans cells were stained with CFW (30 μg/ml) to determine cellular chitin content. After staining for 30 min, the cells were washed and visualized by confocal laser scanning microscopy (CLSM) with a 63× oil objective lens. The fluorescence intensity was recorded using a BioTek H1 plate reader ($\lambda_{excitation}$ = 405 nm and $\lambda_{emmision}$ = 450 nm) to indicate the relative chitin content in the different strains.

Measurement of mannan content

C. albicans cells were stained with concanavalin A (ConA)–FITC (50 μg/ml) for 30 min to determine the α-mannopyranosyl content. After staining, the cells were collected and subjected to flow cytometry to measure fluorescence intensity. A total of 10,000 events were collected for data analysis without using specific gating strategies. The obtained data were analyzed by FlowJo version 10 software. Meanwhile, stained samples were observed by CLSM with a 63× oil objective lens.

β-Glucan exposure assay

To stain β-(1,3)-glucan in the cell wall, exponentially growing *C. albicans* yeast cells or drug-treated cells were washed with PBS, blocked with BSA, incubated with an anti–β-(1,3)-glucan antibody overnight at 4°C, and stained with FITC- or TRITC-labeled goat anti-mouse secondary antibody for 1 hour at 30°C. The stained cells were observed by a Zeiss LSM 700 confocal laser scanning microscope. The fluorescence intensity of the stained cells was detected by flow cytometry. The data were analyzed using FlowJo version 10 software or WinMDI 2.9 software.

Protein extracts and immunoblot assays

C. albicans cells were harvested by centrifugation, washed once with sterile water, and then resuspended in two volumes of lysis buffer [50 mM tris-HCl (pH 7.5), 100 mM NaCl, 0.1% Triton X-100, and 0.1% (w/v) sodium deoxycholate] containing a protease inhibitor cocktail (Roche) and phosphatase inhibitors (50 mM NaF and 100 mM β-glycerophosphate). One cell volume of 0.4-mm glass beads was added before three 60-s rounds of homogenization in a Precellys 24 homogenizer (Bertin Technologies, Montigny le Bretonneux, France). To equalize the amount of protein loaded, the protein concentration was calculated using Bradford reagent (Beyotime, Shanghai, China) with BSA as a standard. The blots were probed with an anti–phospho-p44/p42 MAPK (Thr^{202}/Tyr^{204}) antibody (Cell Signaling Technology) for Cek1-P and Mkc1-P detection. A β-tubulin antibody (Abmart Shanghai Co. Ltd.) was used as internal control.

Transmission electron microscopy

Overnight-grown *C. albicans* cells were harvested by centrifugation and washed with PBS. The pellet was fixed in 2.5% glutaraldehyde at 4°C for 24 hours and then placed in 1% osmium tetroxide in 0.1 M sodium cacodylate at pH 7.4 for 1 hour. The cells were desiccated in graded series of acetone and embedded with EPON-812. Ultrathin sections were prepared and observed under a transmission electron microscope (JEM-1011, JEOL, Tokyo, Japan).

Murine model of OPC

The antifungal activity of PA in vivo was evaluated using an oral infection model. BALB/c male mice (6 to 8 weeks old) were immunosuppressed with two subcutaneous injections of prednisolone at a dose of 100 mg/kg of body weight 1 day before infection with *C. albicans* 28A, an azole-resistant strain originally isolated from a patient who suffered from OPC. The mice received tetracycline hydrochloride in drinking water at a concentration of 0.83 mg/ml beginning 1 day before infection. On the day of infection, the animals were anesthetized by intramuscular injection with 50 μl of chlorpromazine chloride (2 mg/ml) in each femur. Small cotton pads soaked in a *C. albicans* cell suspension (2×10^7 viable cells/ml) were used to swab the entire oral cavity of the anesthetized mice to produce oral infections. One day after infection, PA (300 μg/ml) or EAOA (1 mg/ml) was added to the drinking water of the animals. The mice were euthanized after completing 2 days of therapy, and the tongues were excised and divided longitudinally. One half was weighed and homogenized in PBS for quantitative culture. The other half of the tongue was fixed in zinc-buffered

formalin and embedded in paraffin, after which thin sections were cut and stained with PAS. All treatment groups consisted of five animals.

Ethics statement

The animal experiments in this study were conducted under a protocol authorized by the Animal Care and Use Committee at Shandong University under approval number 2017-D026. Animal experiments were minimized, and the murine research methods were designed to minimize mouse suffering.

Screen for *C. albicans* CBS inhibitors

We screened a compound library including 51,520 synthetic compounds from the Chinese National Center for Drug Screening, more than 200 natural molecules from our laboratory, and two known human CBS inhibitors, i.e., benserazide (*40*) and (−)-gallocatechin gallate (*41*), to identify fungal CBS inhibitors using an in vitro CBS enzyme assay. The reaction was performed in the presence of 50 μl (for high-throughput screening in 384-well plates) or 100 μl (for ordinary screening in 96-well plates) of Na/bicine buffer containing 200 mM Na/bicine (pH 8.6), 50 μM PLP, BSA (0.25 mg/ml), Cys4 (0.2 μg/ml), 10 mM L-cysteine, and 10 mM L-homocysteine as substrates. The inhibitor was added 10 min before substrates at the indicated concentration, and the reaction was allowed to proceed for 120 min at 37°C. Lead acetate was used as a H_2S sensor to assay CBS activity. Lead acetate reacted with H_2S, and the generated product was measured on the basis of the increase in absorbance at 390 nm.

Measurement of the affinity between fungal CBS and its inhibitors

The interaction between AOA/PA and Cys4 was measured using a biolayer interferometry method with Octet RED 96 (ForteBio Inc., CA, USA). The assay was performed at 30°C in PBS (pH 7.4) as the assay buffer. The assay also contained 0.1% BSA and 0.02% Tween 20 to reduce nonspecific interactions and 2% dimethyl sulfoxide to increase compound solubility. Purified Cys4 was biotinylated and coated onto Super Streptavidin Biosensor tips (ForteBio Inc.). The binding experiments with the small molecules were carried out at the indicated concentrations from 3.125 to 300 μM. During the course of the experiment, the sample plates were shaken continuously at 1000 rpm. The binding constants were determined by global fits of the binding curves using the Octet Red software provided by the manufacturer. The resulting data were analyzed on the basis of a 1:1 binding model, and K_d values were calculated.

Time-killing kinetics of the combination of EAOA/PA and H_2O_2 on planktonic *C. albicans* cells

To explore the potentiation of the effects of H_2O_2 on *C. albicans* by EAOA/PA, time-killing curves were plotted by measuring the viability of cells treated with EAOA/PA and H_2O_2 individually or in combination. Exponential-phase SC5314 cells were diluted with SD medium or RPMI 1640 medium. EAOA (40 or 80 μg/ml)/PA (32 or 64 μg/ml), H_2O_2 (5 mM), or both were added and incubated at 30°C. The number of viable cells was determined by a colony-counting method at specific times.

Expression and purification of the catalytic core structure of *C. albicans* CBS

The sequence of cCBS-cc (residues 1 to 319) was amplified from genomic DNA and cloned into pET-32a(+). After sequence confirmation, the resulting vector was used to transform *E. coli* BL21. The expression and purification procedures were conducted as described above. The N-terminal Trx-His tag was removed by thrombin in a dialysis system containing 20 mM tris-HCl (pH 8.0), 200 mM NaCl, 10% glycerol, and 1 mM β-mercaptoethanol. The resulting protein solutions were passed through a Ni-NTA column, leaving the thrombin and Trx-His tag bound on the column. The protein was further purified by a HiTrap ion exchange column (GE Healthcare) with an elution gradient from 0 to 1 M NaCl in 25 mM tris-HCl buffer (pH 8.0). The final purification step was size exclusion chromatography (Superdex 200, GE Healthcare) in 10 mM tris-HCl buffer (pH 8.0) containing 100 mM NaCl.

Crystallization and structure determination

The crystallization and structure determination of cCBS-cc were performed according to our previously reported method (*42*). X-ray diffraction datasets were collected at the Shanghai Synchrotron Radiation Facility beamline BL19U (wavelength, 0.9785 Å). The crystal structure was solved by molecular replacement methods using the program Phaser in the CCP4 program suite with human CBS [Protein Data Bank (PDB) code: 4COO] as the search model. The model was manually completed with COOT and refined with the PHENIX crystallographic software package. The final model had an R_{work}/R_{free} of 0.201/0.258. The quality of the final model was evaluated using MolProbity. Data collection, refinement, and validation statistics are provided in table S3.

Homology modeling

As the crystal structure of *C. albicans* CBS has not yet been resolved, homology modeling was used to construct the full length structure of *C. albicans* CBS. The missing residues in the crystal structure of cCBS-cc were modeled using the MODELLER program, and human CBS (PDB code: 4COO) was used as the template structure for homology modeling. The top-scoring structure was selected for further optimization using SYBYL-X. Hydrogens were added, and all side chains were subjected to 100 steps of minimization using the Powell method. The quality of the homology model was checked using PROCHECK. The established structure is freely available for download at https://doi.org/10.6084/m9.figshare.11919825. To characterize the mode of binding between PA and CBS, molecular docking was performed using AutoDock Vina, and the top-scoring results were selected as the representative model.

Fungal CBS mutants and human CBS

On the basis of the molecular docking between PA and *C. albicans* CBS, Lys^{53} and Asn^{83} were identified as two key amino acid residues that potentially influence the interaction. The sequences encoding the two single mutants and one double mutant of cCBS-cc were synthesized by GENEWIZ (Nanjing, China). The mutants were heterologously expressed in *E. coli*, and their H_2S generation activity was assessed. The sequence encoding human CBS was also synthesized by GENEWIZ and used to transform *E. coli* for protein expression.

Statistical analysis

At least three biological replicates were performed for all experiments unless otherwise indicated. Statistical significance was assessed in GraphPad Prism using log-rank (Mantel-Cox) test for the survival analysis. Other data were statistically analyzed using one-way analysis of variance (ANOVA), followed by Tukey's test for comparing more than two groups or Student's *t* test to compare values between two specific groups. Statistical significance was determined according to the *P* value. $^{*}P < 0.05$, $^{**}P < 0.01$, and $^{***}P < 0.001$; and ns means not significant. Statistical details are found in the figures or figure legends.

Synthesis of EAOA

AOA (1.5 g, 16.5 mmol) was dissolved in ethanol (5 ml) and cooled to 0°C. Hydrogen chloride gas (formed by the addition of H_2SO_4 over HCl) was then bubbled into the mixture, and the resulting yellow solution was allowed to stand at room temperature for 24 hours. The mixture was concentrated in vacuo, and the residue was taken up in Et_2O. After filtration, the white precipitate was collected to give the corresponding product.

Isolation of PA

PA was isolated from the lichen *Nephromopsis pallescens* (Schaer.) Park, which was collected in the Puer region of Yunnan province in China. A sample of the lichen was authenticated by L. Wang of the Kunming Institute of Botany, Chinese Academy of Sciences.

The air-dried and powdered whole parts of *N. pallescens* (158.47 g) were extracted three times with 78% aqueous ethanol at room temperature for 24 hours and then extracted by ultrasonic processing for 30 min at room temperature. After filtration and concentration in vacuo, the ethanol-free residue (70.50 g) was obtained. The extract was subjected to silica gel column chromatography (CC) eluted with a petrol ether–Me_2CO gradient system (9:1, 8:2, and 7:3, v/v) and then a $CHCl_3$-MeOH gradient system (9:1, 8:2, 7:3) to give eight fractions. Fractions 1 to 4 (1.50 g) were subjected to repeated CC over silica gel (petroleum ether:Me_2CO, 92:8) to yield several fractions, which were then subjected to repeated prep-HPLC chromatography to obtain PA (0.45 g). The structure of PA was identified by comparison of its nuclear magnetic resonance and MS data with the previous literature (*43*).

Synthesis of PA-TPP

PA-TPP was synthesized through an esterification reaction using dicyclohexylcarbodiimide (DCC) reagent. Unexpectedly, the C═C double bond of the PA molecule migrated even under mild conditions (DCC-mediated esterification of carboxylic acid and alcohol at ambient temperature).

Supplementary Materials

This PDF file includes:

Figs. S1 to S32
Tables S2 to S4
The PDB file of crystal structure of cCBS-cc under accession code 7XRQ
References

Other Supplementary Material for this manuscript includes the following:

Tables S1 and S5

View/request a protocol for this paper from *Bio-protocol*.

REFERENCES AND NOTES

1. Nature Microbiology Editorial, Stop neglecting fungi. *Nat. Microbiol.* **2**, 17120 (2017).
2. M. C. Fisher, N. J. Hawkins, D. Sanglard, S. J. Gurr, Worldwide emergence of resistance to antifungal drugs challenges human health and food security. *Science* **360**, 739–742 (2018).
3. A. D. S. Dantas, K. K. LEE, I. Raziunaite, K. Schaefer, J. Wagener, B. Yadav, N. A. R. Gow, Cell biology of *Candida albicans*–Host interactions. *Curr. Opin. Microbiol.* **34**, 111–118 (2016).
4. A. J. P. Brown, G. D. Brown, M. G. Netea, N. A. R. Gow, Metabolism impacts upon *Candida* immunogenicity and pathogenicity at multiple levels. *Trends Microbiol.* **22**, 614–622 (2014).
5. A. J. P. Brown, K. Haynes, N. A. R. Gow, J. Quinn, *Stress Responses in Candida* (ASM Press, 2012).
6. G. Yang, L. Wu, B. Jiang, J. Qi, K. Cao, Q. Meng, A. K. Mustafa, W. Mu, S. Zhang, S. H. Snyder, R. Wang, H_2S as a physiologic vasorelaxant: Hypertension in mice with deletion of cystathionine γ-lyase. *Science* **322**, 587–590 (2008).
7. K. Shatalin, E. Shatalina, A. Mironov, E. Nudler, H_2S: A universal defense against antibiotics in bacteria. *Science* **334**, 986–990 (2011).
8. R. Wang, Hydrogen sulfide: The third gasotransmitter in biology and medicine. *Antioxid. Redox Signal.* **12**, 1061–1064 (2010).
9. C. Szabo, C. Coletta, C. Chao, K. Módis, B. Szczesny, A. Papapetropoulos, M. R. Hellmich, Tumor-derived hydrogen sulfide, produced by cystathionine-β-synthase, stimulates bioenergetics, cell proliferation, and angiogenesis in colon cancer. *Proc. Natl. Acad. Sci. U.S.A.* **110**, 12474–12479 (2013).
10. C. D. Mccune, S. Chan, M. L. Beio, W. Shen, W. J. Chung, L. M. Szczesniak, C. Chai, S. Q. Koh, P. T.-H. Wong, D. B. Berkowitz, "Zipped Synthesis" by cross-metathesis provides a cystathionine β-synthase inhibitor that attenuates cellular H_2S levels and reduces neuronal infarction in a rat ischemic stroke model. *Acs Cent. Sci.* **2**, 242–252 (2016).
11. X. Chen, K.-H. Jhee, W. D. Kruger, Production of the neuromodulator H_2S by cystathionine β-synthase via the condensation of cysteine and homocysteine. *J. Biol. Chem.* **279**, 52082–52086 (2004).
12. R. Millikin, C. L. Bianco, C. White, S. S. Saund, S. Henriquez, V. Sosa, T. Akaike, Y. Kumagai, S. Soeda, J. P. Toscano, J. Lin, J. M. Fukuto, The chemical biology of protein hydropersulfides: Studies of a possible protective function of biological hydropersulfide generation. *Free Radic. Biol. Med.* **97**, 136–147 (2016).
13. W. K. Huh, S. O. Kang, Characterization of the gene family encoding alternative oxidase from *Candida albicans*. *Biochem. J.* **356**, 595–604 (2001).
14. F. Ruy, A. E. Vercesi, A. J. Kowaltowski, Inhibition of specific electron transport pathways leads to oxidative stress and decreased *Candida albicans* proliferation. *J. Bioenerg. Biomembr.* **38**, 129–135 (2006).
15. S. Costa-de-Oliveira, B. Sampaio-Marques, M. Barbosa, E. Ricardo, C. Pina-Vaz, P. Ludovico, A. G. Rodrigues, An alternative respiratory pathway on *Candida krusei*: Implications on susceptibility profile and oxidative stress. *FEMS Yeast Res.* **12**, 423–429 (2012).
16. P. Zhang, H. Li, J. Cheng, A. Y. Sun, L. Wang, G. Mirchevska, R. Calderone, D. Li, Respiratory stress in mitochondrial electron transport chain complex mutants of *Candida albicans* activates Snf1 kinase response. *Fungal Genet. Biol.* **111**, 73–84 (2018).
17. A. Pradhan, G. M. Avelar, J. M. Bain, D. S. Childers, D. E. Larcombe, M. G. Netea, E. Shekhova, C. A. Munro, G. D. Brown, L. P. Erwig, N. A. R. Gow, A. J. P. Brown, Hypoxia promotes immune evasion by triggering β-glucan masking on the *Candida albicans* cell surface via mitochondrial and cAMP-protein kinase A signaling. *MBio* **9**, e01318-18 (2018).
18. L. Duvenage, L. A. Walker, A. Bojarczuk, S. A. Johnston, D. M. MacCallum, C. A. Munro, C. W. Gourlaya, Inhibition of classical and alternative modes of respiration in *Candida albicans* leads to cell wall remodeling and increased macrophage recognition. *MBio* **10**, e02535-18 (2019).
19. R. A. Monge, E. Roman, C. Nombela, J. Pla, The MAP kinase signal transduction network in *Candida albicans*. *Microbiology* **152**, 905–912 (2006).
20. M. G. Netea, L. A. B. Joosten, J. W. M. van der Meer, B.-J. Kullberg, F. L. van de Veerdonk, Immune defence against *Candida* fungal infections. *Nat. Rev. Immunol.* **15**, 630–642 (2015).
21. E. R. Ballou, G. M. Avelar, D. S. Childers, J. Mackie, J. M. Bain, J. Wagener, S. L. Kastora, M. D. Panea, S. E. Hardison, L. A. Walker, L. P. Erwig, C. A. Munro, N. A. R. Gow, G. D. Brown, D. M. MacCallum, A. J. P. Brown, Lactate signalling regulates fungal β-glucan masking and immune evasion. *Nat. Microbiol.* **2**, 16238 (2016).
22. T. Chen, J. W. Jackson, R. N. Tams, S. E. Davis, T. E. Sparer, T. B. Reynolds, Exposure of *Candida albicans* β (1,3)-glucan is promoted by activation of the Cek1 pathway. *PLOS Genet.* **15**, e1007892 (2019).
23. R. Banerjee, R. Evande, O. Kabil, S. Ojha, S. Taoka, Reaction mechanism and regulation of cystathionine β-synthase. *Biochim. Biophys. Acta* **1647**, 30–35 (2003).
24. H. Teng, B. Wu, K. Zhao, G. Yang, L. Wu, R. Wang, Oxygen-sensitive mitochondrial accumulation of cystathionine β-synthase mediated by Lon protease. *Proc. Natl. Acad. Sci. U.S.A.* **110**, 12679–12684 (2013).

25. Y. Tu, C. A. Kreinbring, M. Hill, C. Liu, G. A. Petsko, C. D. McCune, D. B. Berkowitz, D. Liu, D. Ringe, Crystal structures of cystathionine β-synthase from *Saccharomyces cerevisiae*: One enzymatic step at a time. *Biochemistry* **57**, 3134–3145 (2018).
26. N. A. Gow, V. D. V. Fl, A. J. Brown, M. G. Netea, *Candida albicans* morphogenesis and host defence: Discriminating invasion from colonization. *Nat. Rev. Microbiol.* **10**, 112–122 (2012).
27. A. da Silva Dantas, A. Day, M. Ikeh, I. Kos, B. Achan, J. Quinn, Oxidative stress responses in the human fungal pathogen, *Candida albicans*. *Biomolecules* **5**, 142–165 (2015).
28. P. Bandyopadhyay, I. Pramanick, R. Biswas, S. Ps, S. Sreedharan, S. Singh, R. S. Rajmani, S. Laxman, S. Dutta, A. Singh, S-Adenosylmethionine-responsive cystathionine β-synthase modulates sulfur metabolism and redox balance in *Mycobacterium tuberculosis*. *Sci. Adv.* **8**, eabo0097 (2022).
29. T. Ida, T. Sawa, H. Ihara, Y. Tsuchiya, Y. Watanabe, Y. Kumagai, M. Suematsu, H. Motohashi, S. Fujii, T. Matsunaga, M. Yamamoto, K. Ono, N. O. Devarie-Baez, M. Xian, J. M. Fukuto, T. Akaike, Reactive cysteine persulfides and S-polythiolation regulate oxidative stress and redox signaling. *Proc. Natl. Acad. Sci. U.S.A.* **111**, 7606–7611 (2014).
30. D. Zhang, I. Macinkovic, N. O. Devarie-Baez, J. Pan, C. M. Park, K. S. Carroll, M. R. Filipovic, M. Xian, Detection of protein S-sulfhydration by a tag-switch technique. *Angew. Chem. Int. Ed. Engl.* **53**, 575–581 (2014).
31. E. Zito, ERO1: A protein disulfide oxidase and H_2O_2 producer. *Free Radic. Biol. Med.* **83**, 299–304 (2015).
32. N. Krishnan, C. Fu, D. J. Pappin, N. K. Tonks, H_2S-induced sulfhydration of the phosphatase PTP1B and its role in the endoplasmic reticulum stress response. *Sci. Signal.* **4**, ra86 (2011).
33. M. Csala, E. Kereszturi, J. Mandl, G. Bánhegyi, The endoplasmic reticulum as the extracellular space inside the cell: Role in protein folding and glycosylation. *Antioxid. Redox Signal.* **16**, 1100–1108 (2012).
34. D. F. Díaz-Jiménez, Fungal mannosyltransferases as fitness attributes and their contribution to virulence. *Curr. Protein Pept. Sci.* **18**, 1065–1073 (2016).
35. S. Shahana, D. S. Childers, E. R. Ballou, I. Bohovych, F. C. Odds, N. A. R. Gow, A. J. P. Brown, New Clox systems for rapid and efficient gene disruption in *Candida albicans*. *PLOS ONE* **9**, e100390 (2014).
36. C. Song, J. Luan, Q. Cui, Q. Duan, Z. Li, Y. Gao, R. Li, A. Li, Y. Shen, Y. Li, A. F. Stewart, Y. Zhang, J. Fu, H. Wang, Enhanced heterologous spinosad production from a 79-kb synthetic multioperon assembly. *ACS Synth. Biol.* **8**, 137–147 (2019).
37. B. Peng, W. Chen, C. Liu, E. Rosser, A. Pacheco, Y. Zhao, M. Xian, Fluorescent probes based on nucleophilic substitution–cyclization for hydrogen sulfide detection and bioimaging. *Chemistry* **20**, 1010–1016 (2014).
38. M. Ugliano, R. Kolouchova, P. A. Henschke, Occurrence of hydrogen sulfide in wine and in fermentation: Influence of yeast strain and supplementation of yeast available nitrogen. *J. Ind. Microbiol.* **38**, 423–429 (2011).
39. Clinical and Laboratory Standards Institute, "Reference method for broth dilution antifungal susceptibility testing of yeasts; approved standard" (CLSI document M27-A3, ed. 3, CLSI, 2008).
40. N. Druzhyna, B. Szczesny, G. Olah, K. Módis, A. Asimakopoulou, A. Pavlidou, P. Szoleczky, D. Gerö, K. Yanagi, G. Törö, I. López-García, V. Myrianthopoulos, E. Mikros, J. R. Zatarain, C. Chao, A. Papapetropoulos, M. R. Hellmich, C. Szabo, Screening of a composite library of clinically used drugs and well-characterized pharmacological compounds for cystathionine β-synthase inhibition identifies benserazide as a drug potentially suitable for repurposing for the experimental therapy of colon cancer. *Pharmacol. Res.* **113**, 18–37 (2016).
41. L. Wang, Y. Zhou, F. Wu, High-throughput screening of natural product inhibitors for cystathionine β-synthase. *Biotechnology* **27**, 167–173 (2017).
42. H. N. Yu, X. Y. Liu, S. Gao, B. Sun, H. B. Zheng, M. Ji, A. X. Cheng, H. X. Lou, Structural and biochemical characterization of the plant type III polyketide synthases of the liverwort *Marchantia paleacea*. *Plant Physiol. Biochem.* **125**, 95–105 (2018).
43. A. M. Sarkale, V. Maurya, S. Giri, C. Appayee, Stereodivergent synthesis of chiral paraconic acids via dynamic kinetic resolution of 3-acylsuccinimides. *Org. Lett.* **21**, 4266–4270 (2019).
44. A. M. Gillum, E. Y. Tsay, D. R. Kirsch, Isolation of the *Candida albicans* gene for orotidine-5′-phosphate decarboxylase by complementation of *S. cerevisiae ura3* and *E. coli pyrF* mutations. *Mol. Gen. Genet.* **198**, 179–182 (1984).
45. W. A. Fonzi, M. Y. Irwin, Isogenic strain construction and gene mapping in *Candida albicans*. *Genetics* **134**, 717–728 (1993).
46. W. Chang, J. Liu, M. Zhang, H. Shi, S. Zheng, X. Jin, Y. Gao, S. Wang, A. Ji, H. Lou, Efflux pump-mediated resistance to antifungal compounds can be prevented by conjugation with triphenylphosphonium cation. *Nat. Commun.* **9**, 5102 (2018).

Acknowledgments: We thank M. Xian of Washington State University for the gift of WSP5 used for H_2S detection and J. Berman of Tel Aviv University and A. J. P. Brown of the University of Aberdeen for providing the plasmids used for strain construction. We appreciate the technical assistance from H. Wang of Shandong University in constructing plasmids using the ExoCET DNA assembly method and D. Zhu of Shandong University in preparing the crystals of *C. albicans* CBS. We are grateful to Q. Qi of Shandong University for providing the purchased chemical library for high-throughput screening. The synchrotron radiation experiment was performed at beamline BL19U of the Shanghai Synchrotron Radiation Facility. **Funding:** This work was supported by grants from the National Natural Science Foundation (nos. 81773786 and 82173703) and the Fund for Innovative Team of Shandong University to H.L. and Natural Science Fund for Excellent Young Scholars of Shandong Province of China (ZR2020YQ63) and Qilu Young Scholars Program of Shandong University to W.C. **Author contributions:** W.C. and H.L. conceived the study and designed the experiments. W.C., M.Z., and X.J. constructed strains and conducted mouse experiments. W.C. and M.Z. performed spot assays, flow cytometry tests, and microscopic observations and analyzed data. W.C., M.Z., X.J., and S.Z. performed high-throughput screening of CBS inhibitors, in vitro enzyme tests, and other in vitro experiments. H.Zhang. isolated the compound PA. H.Zheng. and B.S. synthesized EAOA and PA-TPP. Y.Q. and H.Y. crystallized cCBS-cc and elucidated its structure. X.H. performed homology modeling of *C. albicans* CBS. W.C. and H.L. prepared the figures and wrote the manuscript. **Competing interests:** The authors declare that they have no competing interests. **Data and materials availability:** The atomic coordinates have been deposited in PDB under accession code 7XRQ. The RNA-seq data have been deposited in the GEO under accession number GSE137530. All data needed to evaluate the conclusions in the paper are present in the paper and/or the Supplementary Materials.

Submitted 20 June 2022
Accepted 16 November 2022
Published 16 December 2022
10.1126/sciadv.add5366